AN ABSTRACT OF THE THESIS OF

Munseork Choi for the degree of Doctor of Philosophy in Electrical and Computer Engineering presented on May 29, 2008.

Title: 1/f NOISE OF GaAs RESISTORS ON SEMI-INSULATING SUBSTRATES, AND 1/f NOISE DUE TO TEMPERATURE FLUCTUATIONS IN HEAT CONDUCTION

Abstract approved: _____
Leonard Forbes

This research work focuses on the mechanism of 1/f noise in GaAs resistors on semi-insulating substrates and 1/f noise due to temperature fluctuations in heat conduction in resistors, diodes, and bipolar transistors. The goal of this research is to generate accurate models to explain physical origin of 1/f noise in semi-insulating substrate and semiconductor devices dissipating high power.

The model is based on a distributed equivalent circuit representation of the substrate, and shows that 1/f noise bulk phenomena associated with high resistivity substrates. One consequence of the theory is that in this particular instance Hooge's parameter is given by a formula and it is not an empirical parameter.

Power dissipation at high currents and voltages in semiconductor devices results in significant heat generation and heat conduction towards the heat sink. The device temperature is only an average value and there are as a consequence of

the diffusion equation for heat flow itself temperature fluctuations about this average value. It will be shown that these temperature fluctuations can result in 1/f noise at moderately low frequencies where these frequencies are determined by the physical dimensions over which the heat flows and the diffusion transit time. The results are then related to the shot noise or white noise due to the collector current allowing a determination of the 1/f noise corner frequency.

# 1/f NOISE OF GaAs RESISTORS ON SEMI-INSULATING SUBSTRATES, AND 1/f NOISE DUE TO TEMPERATURE FLUCTUATIONS IN HEAT CONDUCTION

by

Munseork Choi

A THESIS

submitted to

Oregon State University

in partial fulfillment of
the requirements for the
degree of

Doctor of Philosophy

Presented May 29, 2008

Commencement June 2009

Doctor of Philosophy thesis of Munseork Choi presented on May 29, 2008

APPROVED:

---

Major Professor, representing Electrical and Computer Engineering

---

Director of the School of Electrical Engineering and Computer Science

---

Dean of the Graduate School

I understand that my thesis will become part of the permanent collection of Oregon State University libraries. My signature below authorizes release of my thesis to any reader upon request.

---

Munseork Choi, Author

ACKNOWLEDGEMENTS

I would like to express the sincere gratitude to my advisor, Dr. Leonard Forbes for his invaluable advice, and insightful guidance throughout my Ph. D. studies. I especially thank for his solid support and continuous encouragement while I am working in AMD and Micron in San Jose California.

I also thank my committee – Dr. Annette von Jouanne, Dr. Pallavi Dhagat, Dr. Albrecht Jander, and Dr. Mei-Ching Lien for providing excellent advice and guidance throughout this process.

As well, I would like to thank all the people of School of EECS for providing such an excellent education and research environment. I would like to particularly thank Ferne Simendinger for her support and for generously helping me navigate through the school system.

I want to thank the generous financial support provided by Micron Corporation. I thank Cheeboon Law and Chihliang Chen in Micron for making life so enjoyable and being loyal friends in San Jose.

I wish to thank the friends in New Vision Church in Milpitas, California.

I also would like to thank the past and present member of the Corvallis Korean Church. Pastor Hyunchan Lee and his wife Myungju Lee, for making Corvallis my home in God. Seungdo Hong for being my big brother. Gamho Ha for showing me a role model as a leader. Pastor Seongguk Shin for taking care of me when I could not stand up. Professor Woochang Cha for leading our praise song in the service.

I extend my greatest thanks to my family for always encouraging me. My Grand Father, MyungSeob Choi, for giving me the unforgettable love forever. My Grand Mother, Myungsu Hyun, for guiding our family to the Lord. My dad, Taesung Choi, for giving me his love and teaching me how to love my sons. My mom, Mihye Kim, for praying for me, always believing in me and strongly supporting that everything I do is so great! My Father in Law, Jaeryong Lee, for giving me strong supports and trust. My Mother in Law, Kyungwha Jung, for praying for me and showing me strong mother's example. My Big Brother and his wife, Wanseok Choi and Myungju Bang, for encouraging and helping me many times when I was in difficult situation.

I also thank my two sons, Samuel Choi and Joshua Choi for giving me so many joys of life, hopes, and vision.

But in the end, the biggest thanks must go to my wife, Sunah Choi. There isn't sufficient room here to say how much I appreciated having you with me in my life.

TABLE OF CONTENTS

TABLE OF CONTENTS (Continued)

Page

TABLE OF CONTENTS (Continued)

# LIST OF FIGURES

# LIST OF FIGURES (Continued)

Figure Page

LIST OF FIGURES (Continued)

Figure Page

# 1/f NOISE OF GaAs RESISTORS ON SEMI-INSULATING SUBSTRATES, AND 1/f NOISE DUE TO TEMPERATURE FLUCTUATIONS IN HEAT CONDUCTION

## 1. INTRODUCTION

### 1.1. Thesis Organization

Electronic devices and systems exhibit random fluctuations in the voltage or current at their terminals, and these fluctuations are usually referred to as noise. The noise described in this thesis is not due to external disturbance which could be eliminated, but is inherent in the system itself. It originates in the random behaviour of the charge carriers within the electronic components constituting the system. This type of noise gives lots of challenging issues in analog circuit design. Especially, analog circuits operating at low frequency range where 1/f noise is significant, one of the most important design issues is how to minimize the 1/f noise in the circuit. As the process technology migrates from 90nm technology to 50nm technology, the size of the CMOS devices is getting smaller and smaller. This smaller device has often smaller signal to noise ratio. More advanced low noise technology and understanding of semiconductor device noise are required to achieve very small low power devices.

The three most commonly encountered types of noise are thermal noise, shot noise, and 1/f noise. Thermal noise arises from the random velocity fluctuations of the charge carriers in a resistive material. The mechanism is sometimes said to be Brownian motion of the charge carriers due to the thermal energy in the material. Thermal noise is present when the resistive element is in

thermal equilibrium with its surroundings, and is often referred to as Johnson noise.

Schottky discussed shot noise in 1918. Shot noise is frequently encountered in solid state devices. It is associated with the passage of current across a barrier such as the depletion layer of a p-n junction.

1/f noise shows a power spectral density which varies frequency as $|f|^{-\gamma}$, where $\gamma$ usually falls between 0.8 and 1.2. There are various theoretical difficulties associated with the treatment of l/f noise. At present, no entirely satisfactory explanation for the phenomenon exists, although in certain instances specific models have been developed. But it appears that such models have only limited application and do not adequately account for many of the observed 1/f noise waveforms.

It is the aim of this paper to present 1/f noise in semiconductor devices using a model based on a distributed equivalent circuit concept [1] and diffusion equation.

Several specific noise parameters have been reviewed such as equivalent input noise voltage, equivalent input noise current, noise figure in single stage circuits, and noise figure in cascaded circuits in chapter 2.

Noises in semiconductor devices are reviewed in chapter 3. These are basic building blocks in low noise devices and circuit design.

Chapter 4 discusses a new theory to analyze the 1/f noise of GaAs resistors on semi-insulating substrates. The model is based on a distributed equivalent circuit representation of the substrate, and shows that 1/f noise bulk phenomena

associated with high resistivity substrates. One consequence of the theory is that in this particular instance Hooge's parameter is given by a formula which has a simple physical interpretation as the ratio of two charges, the thermal charge developed across the substrate capacitance and the charge associated with ionized donors in the resistor channel with proportional constant which depends on the voltage developed in the semi-insulating substrate and doping concentration of the substrate.

Chapter 5 deals with 1/f noise due to temperature fluctuation in semiconductor devices. Power dissipation at high currents and voltages in semiconductor devices results in significant heat generation and heat conduction towards the heat sink. The device temperature is only an average value and there are as a consequence of the diffusion equation for heat flow itself temperature fluctuations about this average value. It will be shown that these temperature fluctuations can result in 1/f noise at moderately low frequencies where these frequencies are determined by the physical dimensions over which the heat flows and the diffusion transit time.

Chapter 6 summaries the research and presents future research works.

### 1.2. Contribution of This Research

The theory of 1/f noise of semi-insulating material was presented in 1995; L. Forbes, "On the theory of 1/f noise of semi-insulating materials," IEEE Trans. on Electron Devices, Vol. 42, No. 10, pp. 1866-1869, (Oct. 1995).

This theory describes the 1/f noise of semi-insulating materials and is analogous to the Nyquist formula for the white thermal noise or Johnson noise of conductors. The theory was applied to FET's on semi-insulating substrates and GaAs resistors on semi-insulating substrates, respectively;

- **L. Forbes, *M.S. Choi* and K.T. Yan, "1/f NOISE OF GaAs RESISTORS ON SEMI-INSULATING SUBSTRATES," IEEE Trans. on Electron Devices, Vol. ED-43, pp. 622-627 , ( April 1996).**
- **L. Forbes, K.T. Yan and *M.S. Choi*, "1/f NOISE CORNER FREQUENCY OF FET's ON SEMI-INSULATING SUBSTRATES," Ext. Abs. U.S. Conf. on GaAs Manufacturing Technology (MANTECH), New Orleans, pp. 52-55, (May 1995).**

The theory on 1/f noise in electron devices due to temperature fluctuations in heat conduction was presented in 1996;

- **L. Forbes, *M.S. Choi*, "1/f Noise in electron devices due to temperature fluctuations in heat conduction," 54th Annual Device Research Conference Digest, Page: 46-7, June 1996.**

The theory was applied to bipolar transistors and other devices.

- **L. Forbes, *M.S. Choi* and W. Cao, "1/f NOISE IN BIPOLAR TRANSISTORS DUE TO TEMPERATURE FLUCTUATIONS IN HEAT CONDUCTION," Microelectronics Reliability, Vol. 39, No. 9, pp. 1357-1364, Sept. 1999.**

This theory could be used to derive more general equations which can be used as a general measure of the noisiness of system or devices. 1/f noise in electronic devices can be represented in terms of the Hooge parameter $\alpha_H$ of the devices. This theory can contribute to create a unified point of view on device noise.

# 2. NOISE IN CIRCUITS AND NOISE MEASUREMENTS

## 2.1. Introduction

In analog electronic circuits and systems, signals are often corrupted by device electronic noises. To evaluate circuit performance and to compare with other designs, we measure the output noise voltages of the circuit. Circuit noise generation is distributed throughout the system and the output noise voltages are the sum of contributions from all noise generators. In this chapter several specific noise parameters have been reviewed such as equivalent input noise voltage, equivalent input noise current, noise figure in single stage circuits, and noise figure in cascaded circuits. These are useful quantities capable of being measured and serving as comparison indexes. Because noise voltages are often very low, it is not possible to measure noise directly at its source. Noise measurement techniques representing the measured output noise in terms of equivalent input noise were reviewed.

## 2.2. Noise Bandwidth

The high frequency operation of many circuits, especially operational amplifiers plays an important role in many applications. Signal bandwidth of an amplifier is defined as the frequency span between zero frequency and the frequency on the frequency axis where the signal transmission has been reduced by -3 dB from the central or midrange reference value. A -3 dB reduction represents a half loss in the power level and corresponds to a voltage level equal to 0.707 of the voltage at the center frequency reference.

Noise bandwidth is not the same as the signal -3 dB bandwidth. The noise bandwidth is the frequency span of a rectangular shape power gain curve equal in area to the area of the actual power gain versus frequency curve. Noise bandwidth is the area under the power curve, the integral of power gain versus frequency, divided by the peak amplitude of the curve. This can be stated in equation form as

$$Noise\ Bandwidth = \Delta f = \frac{1}{P_o}\int_0^\infty P(f)df \tag{2.1}$$

where P( f ) is the power gain as a function of frequency and $P_o$ is the peak power gain. We usually know the frequency behavior of the voltage gain of the system and since power gain is proportional to the network voltage gain squared, the equivalent noise bandwidth can also be written as

$$Noise\ Bandwidth = \Delta f = \frac{1}{Q_{vo}^2}\int_0^\infty |Q_v(f)|^2 df \tag{2.2}$$

where $Q_{vo}$ is the peak magnitude of the voltage gain and $|Q_v(f)|^2$ is the square of the magnitude of the voltage gain over frequency. Figure 2.1 shows the definition of signal and noise bandwidth.

Let's use the concept of the noise bandwidth to derive the output noise power of an amplifier as shown in Figure 2.2, and assume it has low source impedance so that the equivalent input noise voltage $\overline{Q_{vi}^2}$ determines the output noise performance. Assume that the input spectral density $\overline{Q_{vi}^2}/\Delta f = S_i(f)$ of the input noise voltage is known. The total output noise voltage can be obtained by summing the contribution from output noise spectral density, $S_o(f)$ in each frequency increment $\Delta f$ between zero and infinity to give

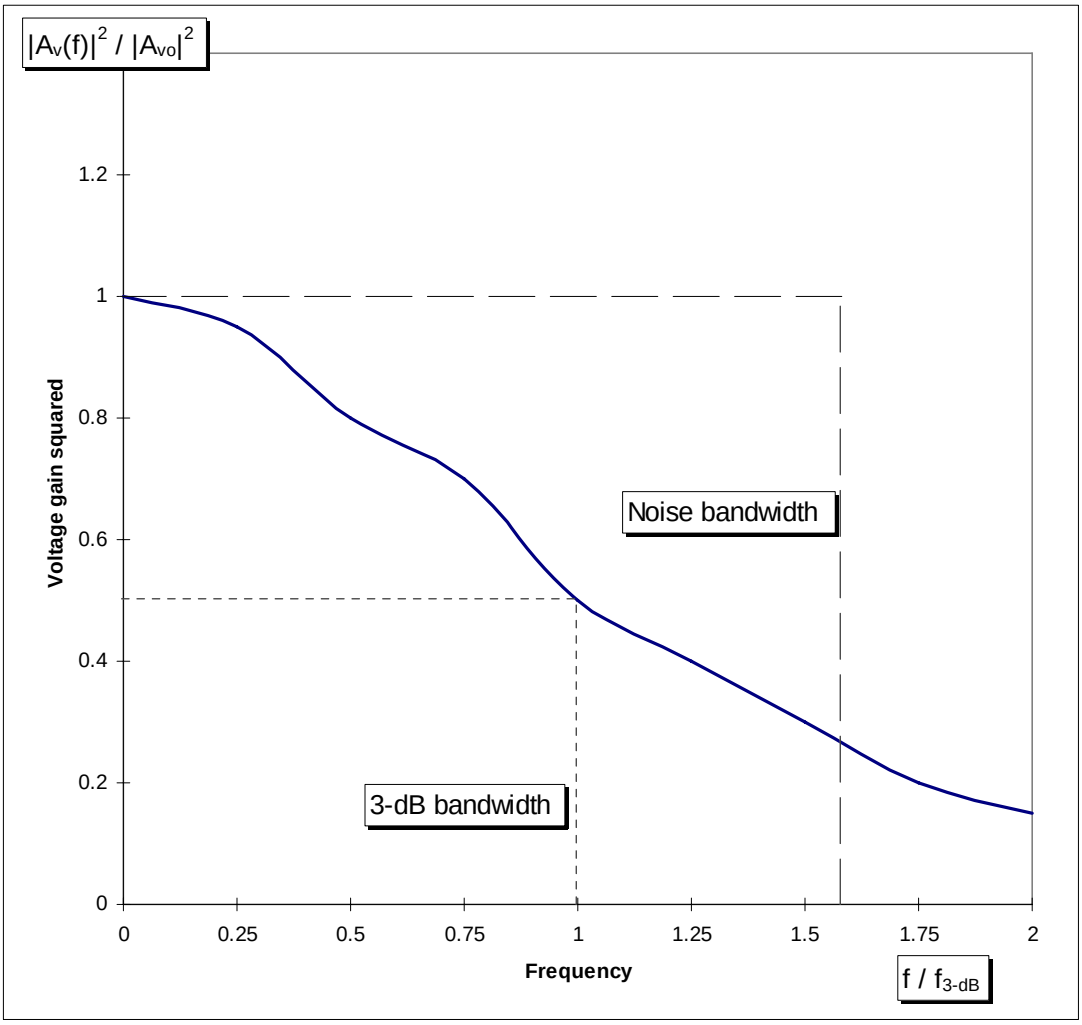


Figure 2.1 Definition of noise bandwidth.

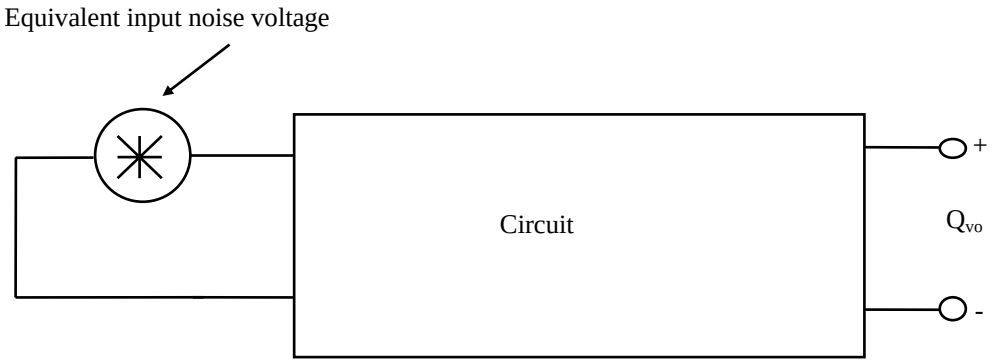


Figure 2.2 Circuit with equivalent input noise voltage generator.

$$\begin{aligned}
\overline{Q_{voT}^2} &= \sum_{f=0}^{\infty} S_o(f)\Delta f = \int_0^{\infty} S_o(f)df = \int_0^{\infty} |Q_v(jf)|^2 S_{io}\,df \\
&= S_{io}\int_0^{\infty} |Q_v(jf)|^2 df \\
&= S_{io}Q_{vo}^2\left[\frac{1}{Q_{vo}^2}\int_0^{\infty} |Q_v(jf)|^2 df\right] \\
&= S_{io}Q_{vo}^2\Delta f
\end{aligned} \tag{2.3}$$

Thus the output noise-voltage spectral density is given by

$$S_o(f) = \overline{Q_{voT}^2}/\Delta f = S_{io}Q_{vo}^2 . \tag{2.4}$$

Equation (2.3) shows that the total output noise of the circuit is easily calculated once we know the noise bandwidth given in the equation (2.2). The equation (2.2) shows that the circuit gain is normalized to its low-frequency value and thus the calculation of noise bandwidth concerns only the frequency response of the circuit. The noise bandwidth can be measured with a calibrated noise generator. The noise generator must be the only significant noise source in the system for this

measurement. First, we can measure the transfer voltage gain $A_{vT}$ at $f_o$ that is the frequency gives the maximum power gain. Then we can measure the total output noise $Q_{vno}$ with the noise generator connected to the input of the system under measurement. The output noise is

$$Q_{vno}^2 = A_{vT}^2 \; Q_{vi}^2 \Delta f \tag{2.5}$$

where $Q_{vi}$ is the input noise signal in volts per hertz $^{1/2}$.

The noise bandwidth can be derived from the above equation (2.5)

$$\Delta f = \left( \frac{Q_{vno}}{A_{vT} \; Q_{vi}} \right)^2 . \tag{2.6}$$

**2.3. Noise Figure and Signal-to-Noise Ratio**

The incoming signal to wireless devices is very weak, and the signal should be amplified to be processed in the next circuit stages of the system. When the weak signal is amplified, the noise associated with the signal is amplified. The amplification system also adds noise to the signal in many cases. The power ratio of the input signal to noise is usually degraded.

The noisiness of a linear system can be evaluated by a noise figure. The noise figure F is a commonly used method of specifying the noise performance of a circuit or a device. It is widely used as a measure of noise performance in communication systems. The noise figure of a two-port device is generally defined by the ratio of the available output noise power per unit bandwidth to the portion of that noise caused by the actual source connected to the input terminals

of the device, measured at the standard temperature of 290 K [13]. This definition of the noise figure in equation form is

$$F = \frac{Total\ available\ output\ noise\ power}{Portion\ of\ \ output\ noise\ power\ due\ to\ the\ source\ resistor}. \qquad (2.7)$$

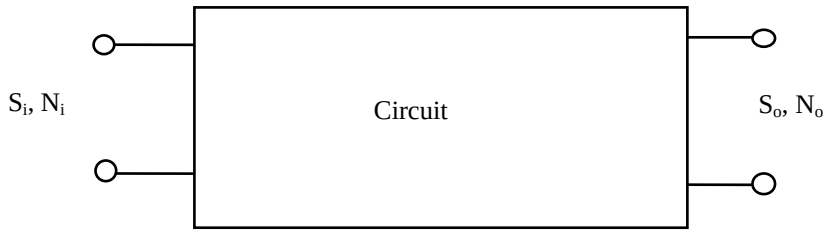


Figure 2.3 Signal and noise power at the input and output of a two-port circuit.

Consider a circuit as shown in Figure 2.3, where S represents signal power and N represents noise power. The input noise power $N_i$ is always taken as the noise in the source resistance. The output noise power $N_o$ is the total output noise including the circuit contribution and noise transmitted from the source resistance. An equivalent definition of the noise figure is

$$F = \frac{Input\ signal-to-noise\ ratio}{Output\ signal-to-noise\ ratio} = \frac{S_i / N_i}{S_o / N_o}. \qquad (2.8)$$

The noise figure, since it is a power ratio, can be expressed in decibels. When expressed in decibels, the logarithmic expression for the noise figure, $F_{DB}$ is

$$\begin{aligned} F_{DB} &= 10\log F \\ &= 10\log\frac{S_i / N_i}{S_o / N_o} = 10\log\frac{S_i}{N_i} - 10\log\frac{S_o}{N_o}. \end{aligned} \qquad (2.9)$$

We can also write $F_{DB}$ in terms of voltage,

$$F_{DB} = 20\log\frac{Q_{vs}}{Q_{vnt}} - 20\log\frac{Q_{vso}}{Q_{vno}} \qquad (2.10)$$

where $Q_{vnt}$ is the input thermal noise voltage and $Q_{vno}$ is the output noise voltage.

The noise figure is a measure of the signal-to-noise degradation after the amplification. For a noise free amplifier, one that adds no noise to the thermal noise of the source, the ideal noise figure is F= 1 and $F_{DB}$ = 0 dB. Noisy system has higher value of noise figure.

To predict ways of minimizing system noise, we can derive an expression for over all noise figure of the system when several amplifiers are connected in cascade.

The system to be analyzed consists of a signal source with internal terminal noise and two cascaded circuits as shown in Figure 2.4.

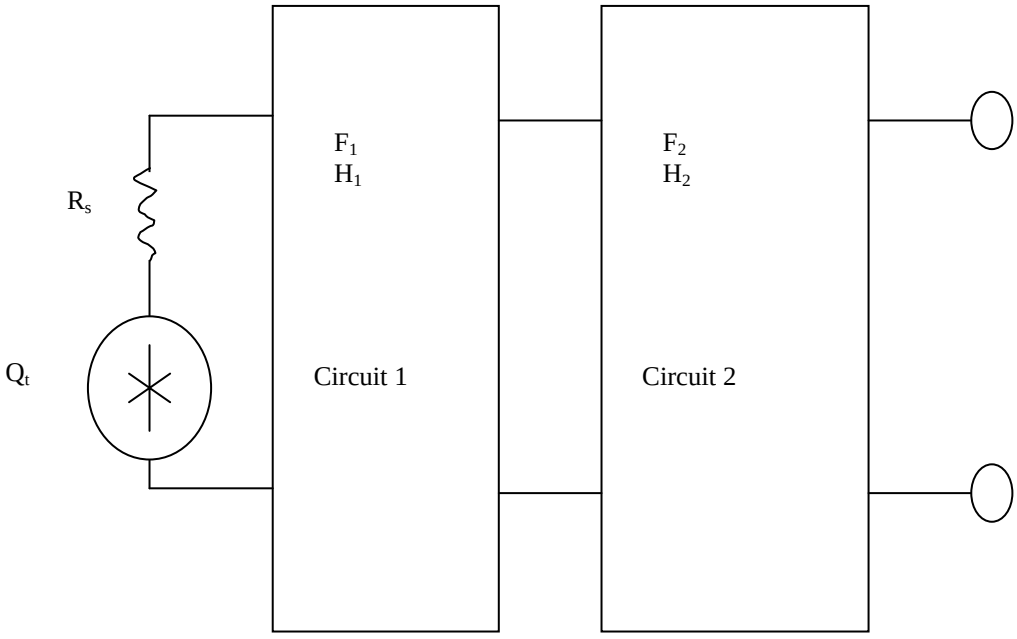


Figure2.4 Two amplifier networks in cascade.

The available power gain of the system is represented by $H_a$, and the available thermal noise power is $P_{ni} = Q_t^2 / 4R_s$. The first stage noise figure $F_1$ is

$$F_1 = P_{no} / H_a kT\Delta f \tag{2.11}$$

where $P_{no}$ is the available noise power at the load terminals. The available noise power at the input to second stage, $P_{ni2}$, is

$$P_{ni2} = P_{no1} = F_1 H_1 kT\Delta f \ . \tag{2.12}$$

The second stage noise figure $F_2$ is

$$F_2 = P_{no2} / H_2 kT\Delta f \ . \tag{2.13}$$

The noise generated in the second stage is $P_{no2} - H_2 kT\Delta f$ , and from the above equation

$$F_2 H_2 kT\Delta f - H_2 kT\Delta f = (F_2 - 1) H_2 kT\Delta f \ . \tag{2.14}$$

The $H_2 kT\Delta f$ term represents the thermal noise power in the source resistance for circuit2. The total output noise $P_{noT}$ is given by

$$\begin{aligned} P_{noT} &= H_2 (F_1 H_1 kT\Delta f) + (F_2 - 1) H_2 kT\Delta f \\ &= (F_1 H_1 H_2 + F_2 H_2 - H_2) kT\Delta f \end{aligned} \ . \tag{2.15}$$

Thus the noise factor of the cascaded two stages is

$$F_{12} = P_{noT} / H_1 H_2 kT\Delta f = F_1 + (F_2 - 1) / H_1 . \tag{2.16}$$

If the analysis is extended to three stages, we obtain the following relation developed by Friis [2]:

$$F_{123} = F_1 + (F_2 - 1) / H_1 + (F_3 - 1) / H_1 H_2 . \tag{2.17}$$

Amplifier noise is represented completely by a zero impedance voltage generator $E_n$ in series with the input port, an infinite impedance current generator

$I_n$ in parallel with the input as shown in Figure 2.5. Each of these terms typically are frequency dependent. The thermal noise of the signal source is represented by the generator $Q_{vt}$. Equivalent input noise, $Q_{vni}$, will be used to refer all three noise sources to the signal source location. The levels of signal voltage and noise voltage that reach $Z_{in}$ in the circuit are multiplied by the noiseless voltage gain $A_v$. For the signal path, the transfer function from input signal source to output port is represented by system gain $A_{vT}$,

$$A_{vT} = Q_{vso} / Q_{vin} = \frac{A_v V_{in} Z_{in}}{R_s + Z_{in}}. \tag{2.18}$$

The total noise at the output port is

$$Q_{vno}^2 = A_v^2 Q_{vi}^2. \tag{2.19}$$

The noise at the input to the amplifier is

$$Q_{vi}^2 = (Q_{vt}^2 + Q_{vn}^2)\left|\frac{Z_{in}}{Z_{in} + R_s}\right|^2 + I_n^2\left|\frac{Z_{in}R_s}{Z_{in} + R_s}\right|^2. \tag{2.20}$$

The total output noise is

$$Q_{vno}^2 = A_v^2(Q_{vt}^2 + Q_{vn}^2)\left|\frac{Z_{in}}{Z_{in} + R_s}\right|^2 + A_v^2 I_n^2\left|\frac{Z_{in}R_s}{Z_{in} + R_s}\right|^2. \tag{2.21}$$

Thus we can get an expression for equivalent input noise, $Q_{vni}^2$

$$Q_{vni}^2 = Q_{vno}^2 / A_{vT}^2 = Q_{vt}^2 + Q_{vn}^2 + I_n^2 R_s^2. \tag{2.22}$$

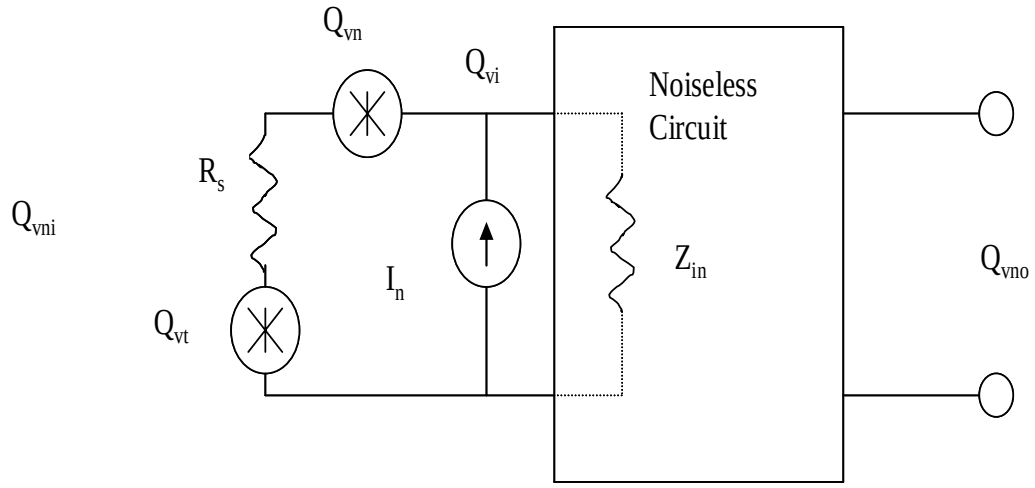


Figure 2.5 Representation of noise in a two-port network by equivalent input voltage and current generators.

The thermal noise of the source resistance is

$$Q_{vt}^2 = 4kTR_s\Delta f \ . \qquad (2.23)$$

If we reduce the source resistance, $R_s$ to small value, then

$$Q_{vni}^2 = Q_{vno}^2 / A_{vT}^2 = Q_{vn}^2$$

the resulting equivalent input noise is the noise generator, $Q_{vn}$. We can find the value for $Q_{vn}$ by dividing total output noise by $A_{vT}$. $I_nR_s$ term is proportional to the value of resistance and contributes a large noise at a sufficiently large value of source resistance.

$$Q_{vni}^2 = Q_{vno}^2 / A_{vT}^2 \cong Q_{vt}^2 + I_n^2R_s^2$$

To find $I_n$, we measure the total output noise with a large source resistance and divide by the system gain if $Q_{vt}^2 << I_n^2R_s^2$. When the InRs term can not be made

dominant, the thermal noise voltage can be subtracted from the equivalent input noise.

## 2.4. Noise Measurement

We have reviewed the equivalent input noise voltage $Q_{vni}$ which is a Thevenin equivalent noise voltage generator located in series with the amplifier impedance and equal to the sum of the amplifier noise. The measurement of equivalent input noise is basic to both the determination of NF and the characterization of the amplifier noise voltage and noise current parameters. The noise measurement of an amplifier system will be considered in this section.

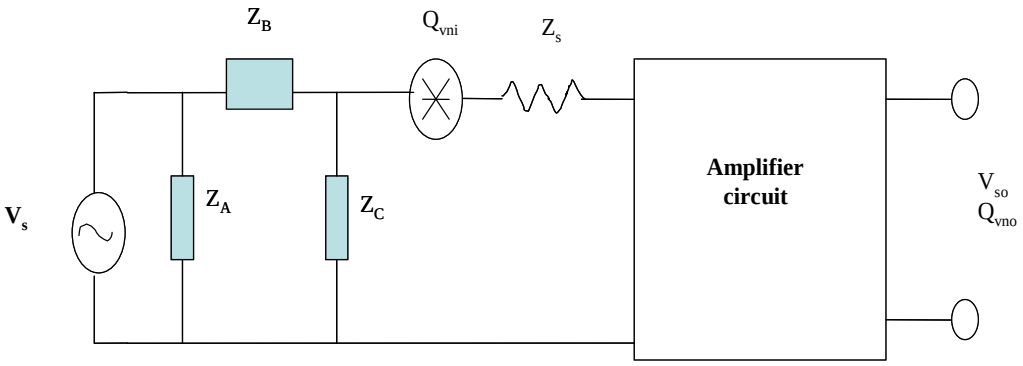


Figure 2.6 Measurement of equivalent input noise using the sine wave method.

We can measure the transfer voltage gain $A_{vT}$ by connecting a voltage generator $V_s$ in series with the source impedance $Z_s$ and measuring the output

signal $V_{so}$ as shown in Figure 2.6. Voltage transfer gain $A_{vT}$ is the ratio of $V_{so}$ to $V_{si}$, $A_{vT} = \frac{V_{so}}{V_{si}}$.

$$V_{so} = A_{vT} \cdot \frac{Z_C}{Z_B + Z_C} . V_s = A_{vT} \cdot V_{si} \tag{2.24}$$

Since this gain must be measured at a signal level higher than the noise level, we have to make sure that the amplifier is biased at a proper voltage level. Low noise amplifier often has high gain, it is necessary to reduce the applied input signal below its minimum setting to avoid overdriving the amplifier by using attenuator. $\frac{Z_C}{Z_B + Z_C} . V_s$ term in equation (2.24) is the voltage reduction after an attenuator inserted between voltage source and amplifier.

The total output noise $Q_{vno}$ is measured to calculate $Q_{vni}$. Remove the signal generator and measure the output noise $Q_{vno}$. The equivalent input noise $Q_{vni}$ is

$$Q_{vni} = \left( A_{vT} \cdot \frac{Z_C}{Z_B + Z_C} \right)^{-1} . Q_{vno} \tag{2.25}$$

To obtain the noise spectral density, divide the equivalent input noise by the square root of the noise bandwidth.

We can measure spectral noise over a wide range of frequencies by using spectrum analyzer. Spectrum measurements show the frequency components that are present in a particular signal. The rms noise is measured in a given noise bandwidth $\Delta f$. The bandwidth of the analyzer changes with the scan range so the noise reading will increase or decrease with noise bandwidth. The correct value is obtained by dividing each reading by the square root of the noise bandwidth $\Delta f$.

When trying to read 1/f noise at low frequencies, the 60 Hz signals and harmonics may be measured, and they look like noise. We can resolve the difference between the pickup and the noise by reducing the scan bandwidth. A simplified noise measurement setup can be constructed with lock-in amplifier that is used as narrow bandwidth frequency tunable RMS voltmeter. We can smooth the meter fluctuations by averaging over a long period of time.

Another method can be used to measure amplifier noise. We can measure calibrated noise source $Q_{vng}$ and output noise measured by a rms output noise meter. The output noise level of the amplifier is compared with the amplitude of the noise generator.

The calibrated noise source is shown in Figure 2.7 as a noise voltage generator in series with the resistance Rs.

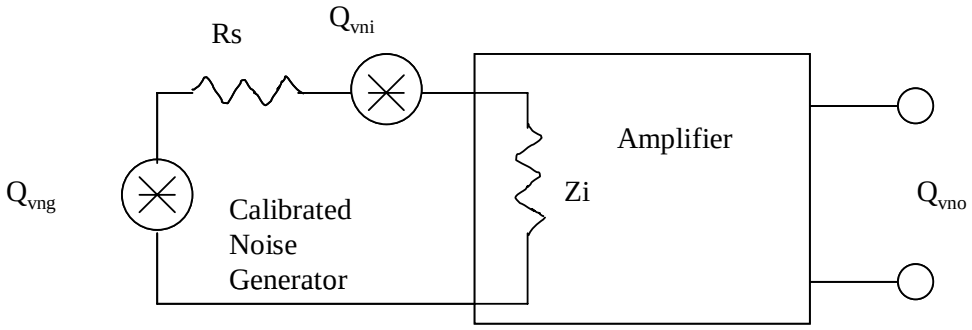


Figure 2.7 Noise generator method for noise measurement.

First, we measure the noise at the output, $Q_{vno1}$ with the generator $Q_{vng}$ connected at the input. Second, we measure the noise at the output, $Q_{vno2}$ without the noise generator at the input.

$$Q_{vno1}^2 = A_{vT}^2\left(Q_{vng}^2 + Q_{vni}^2\right) \tag{2.26}$$

and

$$Q_{vno2}^2 = A_{vT}^2 Q_{vni}^2 \tag{2.27}$$

where $A_{vT}$ is the transfer voltage gain.

From the above two equations, we can calculate $A_{vT}$ and $Q_{vni}$,

$$A_{vT}^2 = \frac{Q_{vno1}^2 - Q_{vno2}^2}{Q_{vng}^2} \tag{2.28}$$

$$Q_{vni}^2 = \frac{Q_{vno2}^2}{A_{vT}^2} = \frac{Q_{vno2}^2 Q_{vng}^2}{Q_{vno1}^2 - Q_{vno2}^2}. \tag{2.29}$$

Third, we increase the noise voltage of the noise generator $Q_{vng}$ to double the output noise power,

$$Q_{vno1}^2 = 2Q_{vno2}^2. \tag{2.30}$$

By substituting this equation (2.30) into the equation (2.29), we find that the noise voltage of the noise generator to double the output noise power is equal to the equivalent input noise of the amplifier,

$$Q_{vni}^2 = \frac{Q_{vno2}^2 Q_{vng}^2}{2Q_{vno2}^2 - Q_{vno2}^2} = Q_{vng}^2. \tag{2.31}$$

## 2.5. Carson's Theorem

This theorem was used to derive 1/f noise equations due to heat conduction in Chapter 5. This theorem is summarized here for readers convenience. The sum of a large number of independent events $H_i(t)$ occurring at random at the average rate $\beta$ is defined as a stationary random variable G(t). An event H(t) starting at

$t=t_i$ can be represented as $H(t-t_i)$. If we assume the event H(t) starts only after time $t_i$, the following equation can be given

$$G(t)=\sum_i H(t-t_i) \tag{2.32}$$

where $H(t-t_i)=0$ for $t < t_i$.

The Fourier transform $\gamma(f)$ of H(u) is

$$\gamma(f)=\int_{-\infty}^{\infty} H(u)\exp(-j\omega u)du \tag{2.33}$$

Then, for sufficiently large T

$$\begin{aligned} a_n &= \frac{1}{T}\int_0^T H(t-t_i)\exp(-j\omega_n t)dt \\ &= \frac{\exp(-j\omega_n t_i)}{T}\int_{-t_i}^{T-t_i} H(u)\exp(-j\omega_n u)du \\ &= \frac{\exp(-j\omega_n t_i)}{T}\int_{-\infty}^{\infty} H(u)\exp(-j\omega_n u)du \\ &= \frac{\exp(-j\omega_n t_i)}{T}\gamma(f_n) \end{aligned} \tag{2.34}$$

The spectral intensity of a single event occurring at $t=t_c$ in $0 \le t \le T$ is

$$S_c(f_n) = 2a_n a_n^* T = \frac{2|\gamma(f_n)|^2}{T}. \tag{2.35}$$

But there are $\beta T$ events in the interval $0 \le t \le T$ and the spectral intensity $S_g(f)$ of G(t) is

$$S_g(f) = \beta T S_c(f) = 2\beta|\gamma(f)|^2 \ . \tag{2.36}$$

The average value of $|\gamma(f)|^2$ , $\overline{|\gamma(f)|^2}$ must be used in eq. (2.39) when $\gamma(f)$ may be different for different individual events

$$S_g(f) = 2\beta\overline{|\gamma(f)|^2}\,. \qquad (2.37)$$

Thus the spectrum density is twice of the Fourier transform $\gamma(f)$ of H(u) times the average rate $\beta$.

# 3. NOISE IN SEMICONDUCTOR DEVICES

## 3.1. Introduction

In the previous chapter topics regarding noises in the circuit and system level were reviewed. Noises in semiconductor devices will be reviewed in this chapter. Five main types of fundamental noise mechanisms are thermal noise, shot noise, generation-recombination noise, random telegraph noise (RTS), and low frequency (1/f) noise. Thermal noise is the most often encountered and will be considered first. A special case of thermal noise limited by shunt capacitance called kT/C noise is also reviewed. The other types of noise are explained in later sections of this chapter.

## 3.2. Thermal Noise

The random fluctuations of the charge carriers in a conductor at a temperature above absolute zero introduce a current fluctuation. Current consists of electrons randomly moving in the material, and each electron carries a charge of $1.602 \times 10^{-19}$ C. Even if the average current in the conductor resulting from these random motions is zero, there is a current fluctuation that results in a voltage fluctuation across the terminals of the conductor. This charge carrier movement is similar to the Brownian motion of particles. J. B. Johnson of Bell Laboratories first observed the thermal noise in 1927 [3], and H. Nyquist presented a theory on thermal noise in 1928 [4].

The thermal noise theory is summarized and reviewed in this section. Two equal resistors $R_1=R_2=R$ are connected across both end of a long transmission line

in parallel. These two resistors are assumed to be at the same temperature T. If the available noise power generated by $R_1$ has a mean square value $\overline{Q_{v1}^2}$, then the power delivered by $R_1$ to $R_2$ is $\overline{Q_{v1}^2}/(4R_1)$. The same amount of power will be delivered by $R_2$ to $R_1$ in thermal equilibrium condition. The transmission line has length D, and characteristic impedance which is equal to R as shown in Figure 3.1. The wave velocity on the transmission line is v. If S(f) is the power spectrum of the open-circuit voltage fluctuations, the mean power delivered by one resistor to the line in a frequency interval $\Delta f$ is

$$\Delta P = \frac{1}{4R} S(f)\Delta f. \tag{3.1}$$

After a wave traveling time from one side of transmission line to the other side, D/v a state of equilibrium is reached in which a mean power $\Delta P$ given by above equation is flowing from left to right and an equal power from right to left. The energy in the transmission line associated with $\Delta f$ is therefore

$$\Delta U = \frac{2D}{v}\Delta P = \frac{D}{2vR} S(f)\Delta f. \tag{3.2}$$

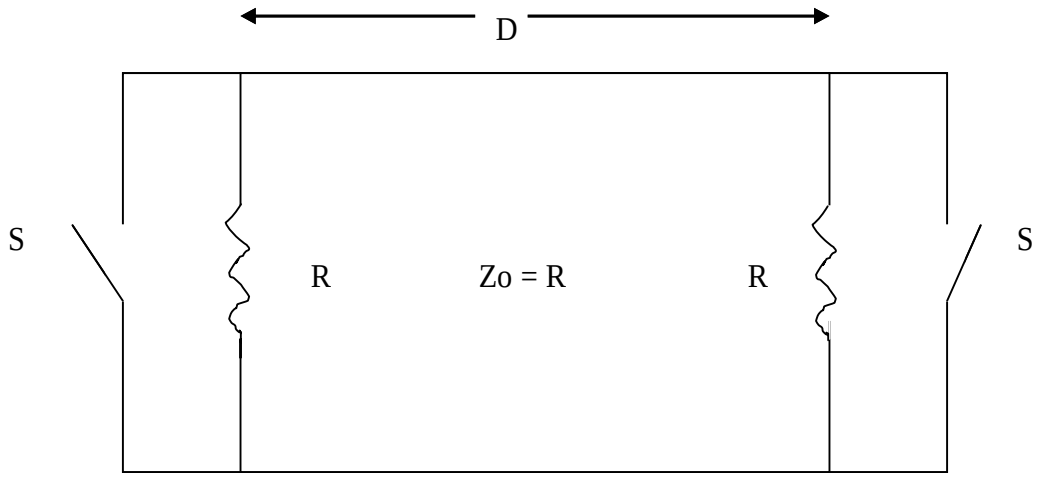


Figure 3.1 Two resistors R in parallel with switch S are connected by means of a lossless transmission line of length l and characteristic impedance Zo=R.

If the transmission line is now shorted at both ends this energy is trapped as standing waves. At each normal mode of the line of frequency f, the trapped energy is

$$E = \frac{hf}{\exp\left(\frac{hf}{kT}\right) - 1} \approx kT \quad if \quad hf << kT. \tag{3.3}$$

where k is Boltzmann's constant (1.38 x $10^{-23}$ W-s/K), T is the temperature of the conductor in Kelvin (K).

The normal modes of the shorted line are given by

$$f = nv / 2D, \tag{3.4}$$

where n is an integer. Thus if D is large, the number of modes in $\Delta f$ is

$$n = \frac{2D}{v} f, \tag{3.5}$$

$$\Delta n = \frac{2D}{v}\Delta f, \tag{3.6}$$

and the mean thermal energy in $\Delta f$ can be calculated

$$\Delta U = \Delta nkT = \frac{2D}{v}kT\Delta f. \tag{3.7}$$

Equation (3.2) and (3.7) describes the same energy $\Delta U$ in the line associated with

$$\frac{D}{2vR}S(f)\Delta f = \frac{2D}{v}kT\Delta f.$$

Therefore the power spectrum of the open-circuit voltage fluctuations is

$$S(f) = 4kTR. \tag{3.8}$$

As shown above, Nyquist's theorem for the thermal noise of a resistance R at a temperature T led to the following expression for the available thermal noise power

$$S_v(f) = \frac{\overline{Q_{vn}^2}}{\Delta f} = 4kTR \tag{3.9}$$

$$S_I(f) = \frac{\overline{Q_{in}^2}}{\Delta f} = 4kT \ / \ R \tag{3.10}$$

where $\Delta f$ is the noise bandwidth of the measuring system in hertz.

A circuit with infinite resistance can not generate an infinite noise voltage, although the thermal noise is proportional to resistance, since there is always some shunt capacitance that limits the voltage across the large resistor. Consider the circuit having resistor-shunt capacitor combination as shown in Figure 3.2.

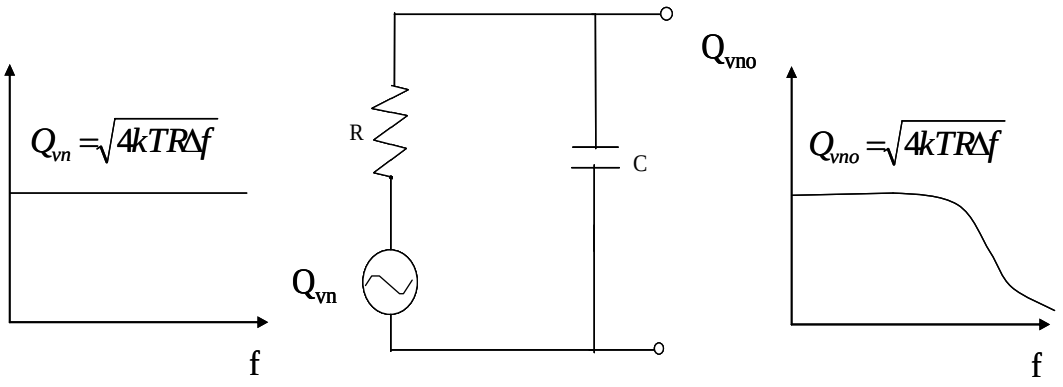


Figure 3.2 Thermal noise of a resistor connected in parallel with shunt capacitor.

The thermal noise voltage is proportional to the square root of the resistance, $Q_{vn} = \sqrt{4kTR\ \Delta f}$ . This RC low pass circuit passes low frequency noise from $Q_{vn}$ to the output noise voltage $Q_{vno}$, but significantly decreases higher frequency components from $Q_{vn}$. The total output noise voltage across the capacitor is

$$\begin{aligned} Q_{vno}^2 &= \int_0^\infty Q_{vn}^2 \left| \frac{1/\ j\omega C}{R + 1/\ j\omega C} \right|^2 df \\ &= \int_0^\infty \frac{Q_{vn}^2}{1 + (\omega RC)^2} df \end{aligned} \tag{3.11}$$

$$\overline{Q_{vno}^2} = \frac{kT}{C} \ . \tag{3.12}$$

Note that the output rms noise voltage is independent of the source resistance and only depends on the temperature and capacitance. The noise per unit bandwidth increases with larger resistance but the band width of the circuit decreases. This noise is called kT/C noise. At a given temperature, this kT/C noise can be reduced by increasing capacitance. It becomes important in applications

and gives many design challenges in designing sigma delta analog-to-digital converters and switched capacitor circuits.

### 3.3. Shot Noise

The movement of minority or majority carriers in the transistors, diodes, and field effect transistors due to drift by electric field and diffusion by gradient of doping concentration contributes to current flow. Each electron and hole carry a charge crosses the potential barrier of p-n junction. Each carrier contributes to a pulse of current. Therefore, total current in a device is the sum of these individual pulses. Fluctuations around the average current I generate $S_I = 2qI$ where q is the electronic charge (1.602 x $10^{-19}$ C). The shot noise current is proportional to the square root of the noise bandwidth. This means that it is white noise containing constant noise power per hertz of bandwidth.

### 3.4. Generation-Recombination Noise

The number of electrons in the conduction band and holes in the valence band may fluctuate because of generation and recombination processes between the band and traps. The generation and recombination is significant when the Fermi level is close to the location of the trap or the center in the forbidden gap. The number fluctuations cause fluctuations in the conductance G, and, therefore, in the resistance *R* [5].

$$\frac{S_R}{R^2} = \frac{S_G}{G^2} = \frac{S_N}{N^2} = \frac{\overline{(\Delta N)^2}}{N^2} \frac{4\tau}{1+\omega^2\tau^2} \tag{3.13}$$

where $\tau$ is a relaxation time, characteristic of the trap, usually in the range of $10^{-6}$ s to $10^{-3}$ s.

The electron traps or donor atoms in the channel of JFET can be a source of the number fluctuation in the channel if these recombination and generation centers can capture or release electrons and holes at the given temperature. This fluctuation explains generation-recombination noise in JFETs.

### 3.5. Random Telegraph Noise (RTN)

In a MOSFET random telegraph noise based on single electron capture and emission events at the oxide and substrate interface was reported [6]. Channel length dependence, or gate bias and geometry dependence of random telegraph signal in MOS were studied [7] [8]. Fluctuations of the threshold voltage, $V_T$ due to RTN have been observed in flash memory arrays. The schematic representation of a flash core cell with an electron trap in the tunneling gate oxide is shown in Figure 3.3.

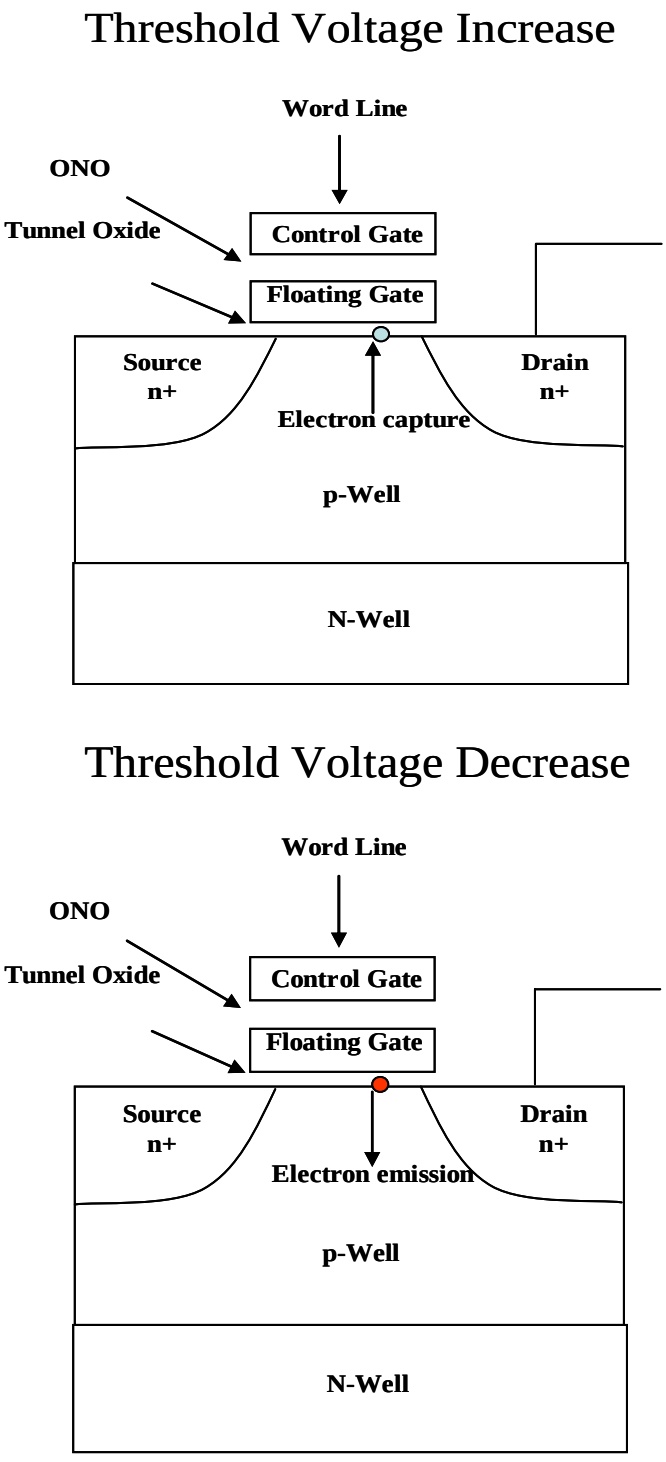


Figure 3.3 Charge trapping and detrapping at the interface of gate oxide and substrate.

The fluctuations of $V_T$ are responsible for drain current instabilities between subsequent memory cell read and verify operations. Drain current versus gate bias voltage due to threshold voltage change is given in Figure3.4.

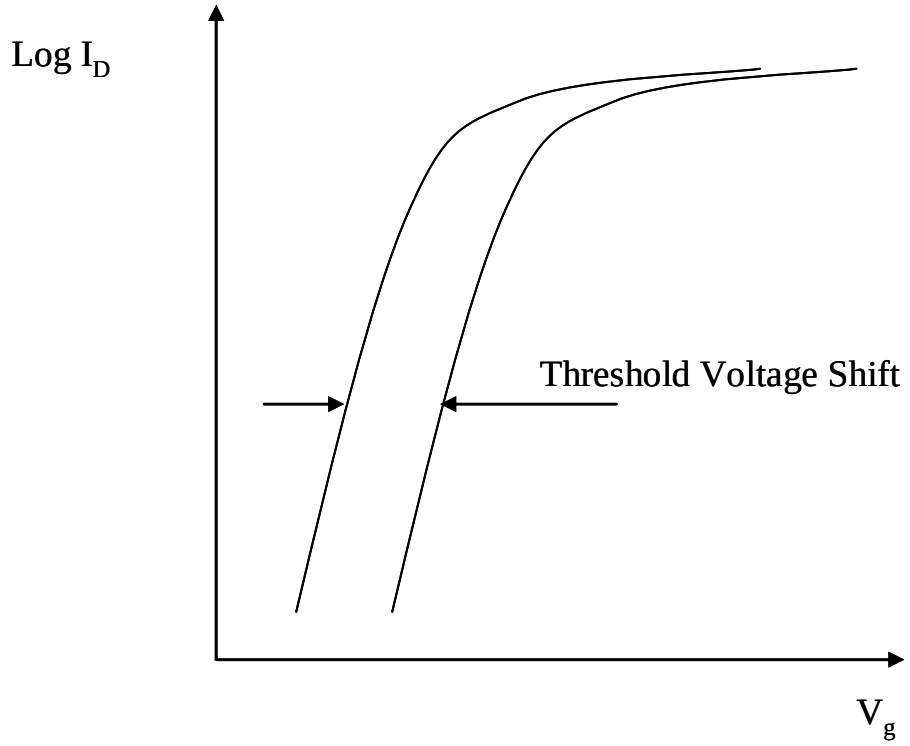


Figure 3.4 Drain current change due to threshold voltage shift.

Because of the very small gate oxide capacitance due to the thicker tunnel oxide, floating gate cell in flash memory shows larger amplitude of threshold fluctuation than CMOS logic devices. Cell size shrinking under sub 90 nm flash memory technology shows increases of RTN noises in memory operations. This threshold voltage fluctuation gives impacts and challenges in designing multi level flash memory core cell. As flash memory core cell sizes are aggressively scaled down, the number of stored electrons in each floating gate greatly reduced. A single

charge trapping and detrapping will induce a significant fluctuation in cell current. Random telegraph noise in drain current of flash core cell is shown in Figure 3.5.

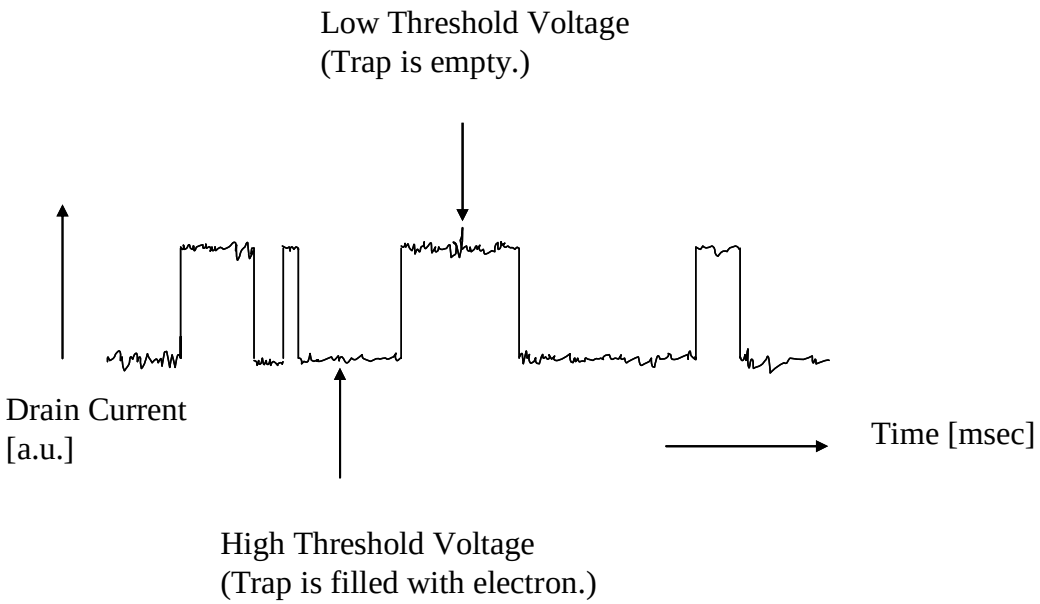


Figure 3.5 RTN noise in drain current.

Stable and fixed cell current at different process corner variation is very critical to distinguish multiple levels of threshold voltage in advanced multi level flash core cell. Threshold voltage levels in single bit flash memory, and 2 bit and 4 bit multi level flash memory cells are given in Figure 3.6.

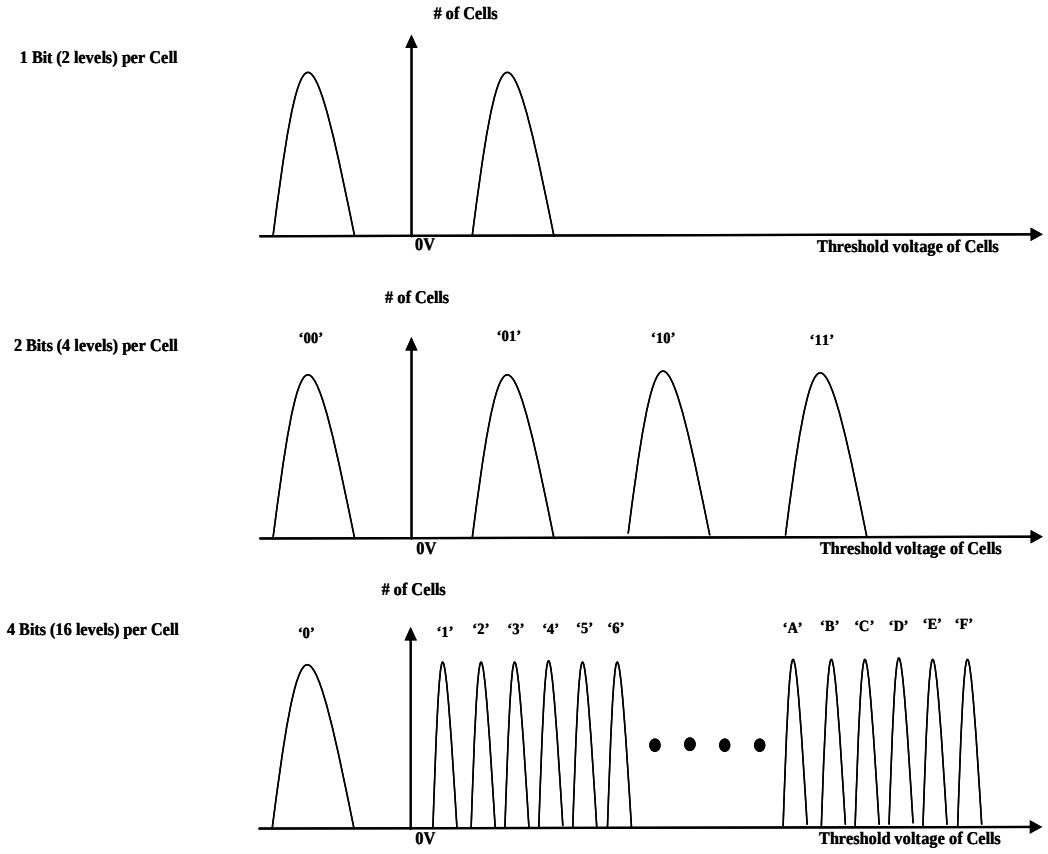


Figure 3.6 Threshold voltage in single and multi level flash memory.

Recently, a lot of attention have been devoted to the RTN research in flash memory cell design. Especially, NAND or SONOS multilevel flash memory cells are under intense research because multi bit per cell is the most efficient way to reduce cost per each die and to overcome the limitation of cell size scaling down. The cross sections of NAND flash memory and SONOS flash memory core cell are given in Figure 3.7 and Figure 3.8 , respectively.

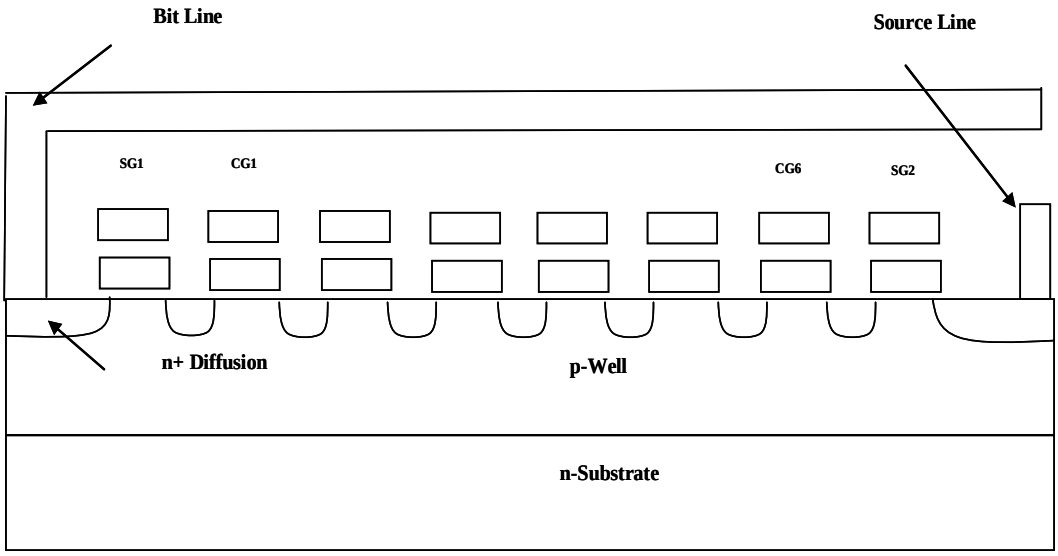


Figure 3.7 NAND flash memory core cell.

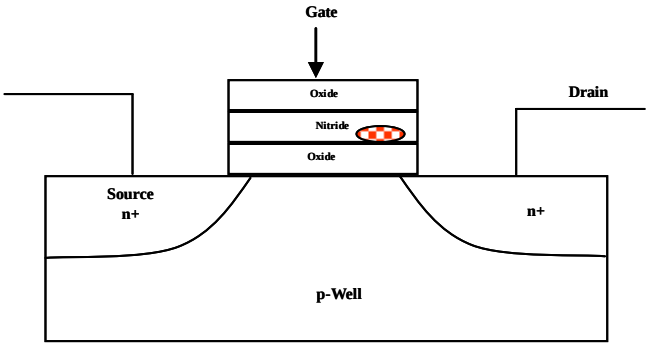


Figure 3.8 SONOS flash memory core cell.

Developing model for the description and quantitative assessment of the threshold voltage variation due to RTN in flash memory arrays was reported [9].

Statistical study to predict the probability for random telegraph noise fluctuations and spectroscopic analysis of the defects contributing to RTN was presented [10].

To model the time behavior of the RTN waveform, a stochastic evolution of a two-

state Markov process was considered under the reasonable assumption that trapping and detrapping dynamics are not history dependent [11].

### 3.6. Flicker Noise or 1/f Noise

The spectral density of low-frequency or 1/f noise increases as frequency decreases. The noise power typically follows a $f^{-\alpha}$ characteristic with $\alpha$ usually unity, but has been observed to take on values from 0.8 to 1.3 in various devices. Unlike other noise sources mentioned above, which are well understood, the origin of the 1/f noise is still open to debate.

Since 1/f noise power is inversely proportional to frequency, it is possible to determine the noise content in a frequency band by integration over the range of frequencies. The result is

$$P_{nf} = \Phi \int_{f_1}^{f_2} \frac{df}{f} = \Phi \ln \frac{f_2}{f_1} \tag{3.14}$$

where $P_{nf}$ is the noise power in watts, $\Phi$ is a dimensional constant also in watts, and $f_1$ and $f_2$ are the lower and upper frequency limits of the band being considered

In 1969, Hooge [12] had postulated the relation

$$\frac{S_R}{R^2} = \frac{\alpha_H}{f\ N} \tag{3.15}$$

in an effort to systematically collect data on 1/f noise from the literature. The only theoretical idea behind the relation was, that whatever the electrons do when producing 1/f noise, they do it independently. Thus, $\alpha_H$ is a normalized measure for the relative noise in different materials, at different temperatures, etc. $\alpha_H$ takes $2 \times 10^{-3}$ as an average value, but it depends on the quality of the crystal, and

on the scattering mechanisms that determine the mobility $\mu$. The near constancy of $\alpha_H$ suggests that this 1/f noise is due to fundamental mechanism of unknown origin; this is useful information that will be found to be valid in other situations as well. It is now generally conceded that $\alpha_H$ is not a universal constant but can be 2 or 3 orders of magnitude lower in perfect material than the $2 \times 10^{-3}$ originally proposed and can be several orders of magnitude smaller than $2 \times 10^{-3}$ for short devices.

# 4. 1/f NOISE OF GaAs RESISTORS ON SEMI-INSULATING SUBSTRATES

## 4.1. Introduction

The solution to this problem, 1/f noise of devices on semi-insulating materials has been suggested by the equivalent circuit techniques of C. T. Sah [14], [15]. These equivalent circuit concepts have been able to reproduce a number of very elegant solutions to difficult problems in conduction in semiconductors and frequency response [16], [17]. These techniques have been applied most recently to develop a theory for the 1/f noise of semi-insulating materials [18].

A distribution of R-C time constants [19] or distributed RC line [20], [21] has previously been suggested as an explanation of 1/f noise. The equivalent circuit technique gives such a distribution of R-C time constants and distributed RC line and relates these directly to parameters of the devices. The semi-insulating substrate is represented by a distributed transmission line and parameters of the line determined by the characteristics of the substrate [18].

GaAs resistors fabricated on semi-insulating substrates [22] exhibit large amounts of 1/f noise at low frequencies. GaAs MESFET's fabricated on semi-insulating substrates are another obvious application of this analysis and the case of most practical interest is that with the FET biased in the saturation region [23], [24] resulting in current injection into substrate, a disturbance in the substrate and consequently noise. Even without current injection the substrate will have thermal noise, at very low frequencies just given by the Nyquist formula and the resistance

of the substrate [18]. The cases where there is just thermal noise of the substrate have not yet been treated in detail and will not be considered here.

This report gives an alternative analysis of published data on GaAs resistors with large applied bias [22] and consequently current injection into the semi-insulating substrate. Since there is some question about the experimental procedures regarding substrate contacts in the original report [22], we have also made our own measurements on implanted GaAs resistors with and without substrate contacts and have included these here.

### 4.2. The Theory of the 1/f Noise of Semi-Insulating Materials

The basic background material for the case where there is current injected into the semi-insulating substrate has been given elsewhere [18] but will be repeated here for convenience of the reader. The semi-insulating substrate is represented using equivalent circuit techniques and there is current injection into the very high impedance and resistance of the substrate. The case where there is no current injection or just thermal noise is not considered here [18]. Figure 4.1 shows in each volume element, dx, the elements $C_n$ and $R_n$ associated with the free carriers. The resistance $R_n$ is large and above the dielectric relaxation frequency is significant, and $C_n$ represents the capacitive effects associated with the redistribution of carriers. Then where all symbols have their usual meanings [14], [16]-[18]

$$R_n = \frac{dx}{q\ \mu\ n\ A} \quad \Omega \tag{4.1}$$

$$C_n = \frac{q^2\ n\ A\ dx}{k\ T} \quad F \tag{4.2}$$

The equivalent transmission line problem for the impedance seen looking into the semi-insulating material is shown in Figure 4.1. In this case both the characteristic impedance and propagation constant are both complexes, neither being real nor imaginary,

$$Z_o = \sqrt{\frac{Z}{Y}} = \sqrt{\frac{R_n}{j\omega\ C_n}} \tag{4.3}$$

$$Z_o = \frac{1}{\sqrt{j\omega}} \sqrt{\frac{(\frac{k\ T}{q})}{\mu}}\ \frac{1}{q\ n\ A} \quad --------\Omega \tag{4.4}$$

$$\gamma\ dx = \sqrt{Z\ Y} = \sqrt{j\omega\ C_n\ R_n}\ \ dx \tag{4.5}$$

$$\gamma\ = \sqrt{j\omega}\ \sqrt{\frac{1}{\frac{k\ T}{q}\ \mu}} \quad ------------cm^{-1} \tag{4.6}$$

For a short line of length l, where the sample is small in the extent or DC frequency the sending end impedance is,

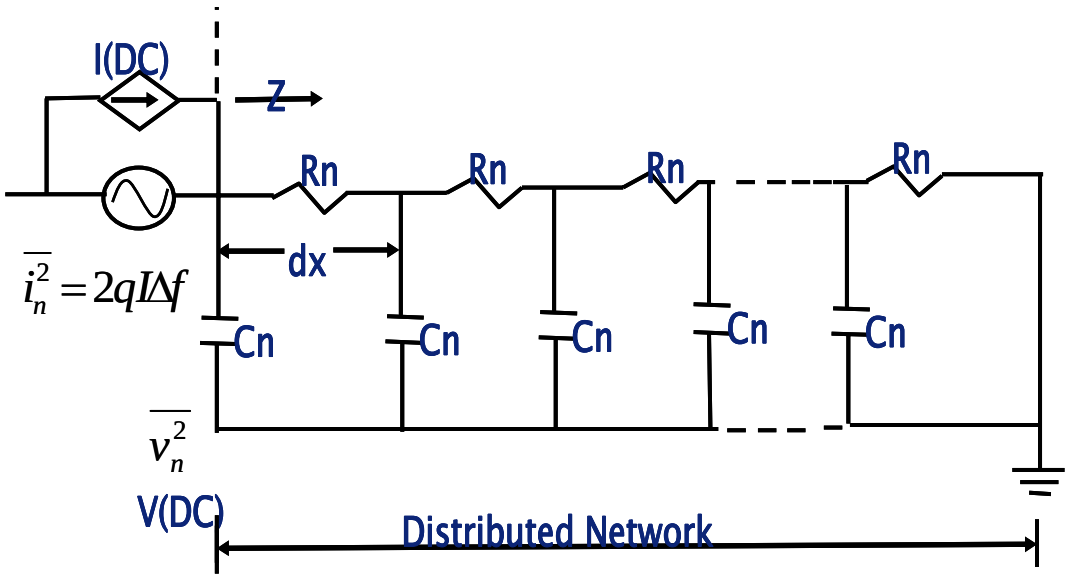


Figure 4.1 Transmission line problem for current injection into semi-insulating material.

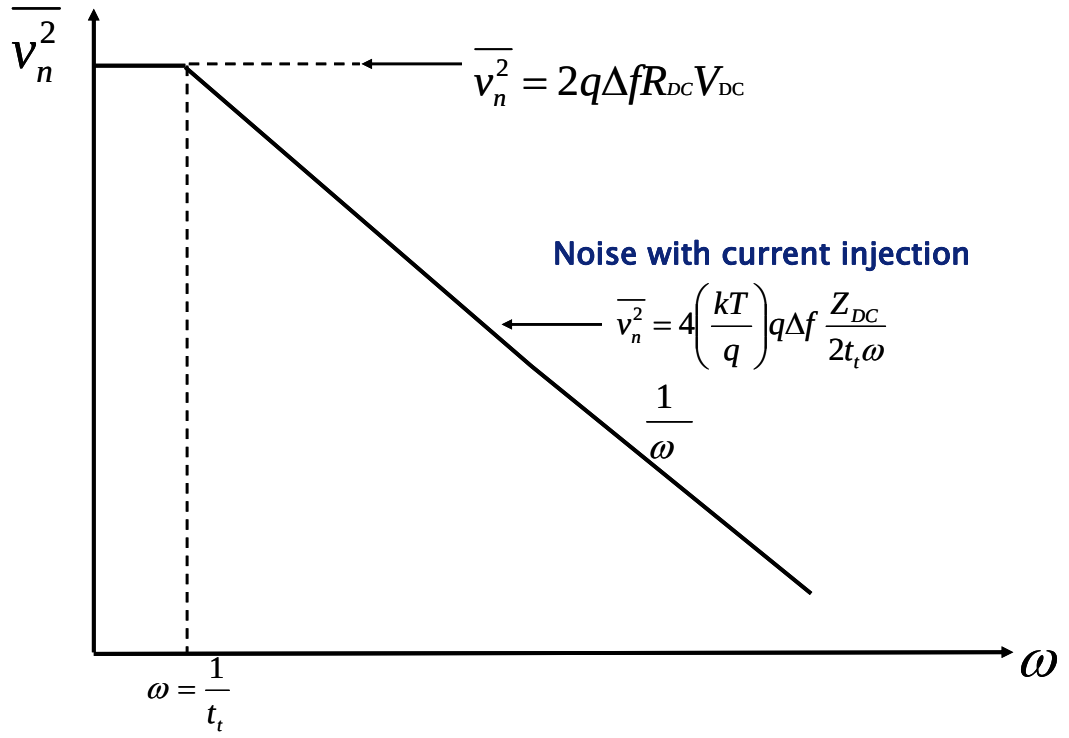


Figure 4.2 Mean square noise voltage due to current injection into semi-insulating material.

$$Z = Z_o \tanh(\gamma\, l) = Z_o\, \gamma\, l \qquad \Omega \tag{4.7}$$

which simplifies to,

$$Z = Z_{DC} = R = \frac{l}{q\, \mu\, n\, A} \qquad \Omega \tag{4.8}$$

or just the DC resistance of the sample.

For long lines of larger extent or frequencies above DC then sending end impedance of this lossy line is just

$$Z = Z_o = \frac{Z_{DC}}{\gamma\, l} \qquad \Omega \tag{4.9}$$

If as shown in Figure 4.1 we now inject a DC current I into this semi-insulating material, there will be a shot noise source with mean square noise current

$$\overline{i_n^{\,2}} = 2\, q\, I\, \Delta f \qquad ----------A^2 \tag{4.10}$$

This mean square noise current will result in a mean square noise voltage at the point of injection;

$$\overline{v_n^{\,2}} = \overline{i_n^{\,2}}\, |Z|^2 \qquad ----------V^2 \tag{4.11}$$

$$= \frac{2\, q\, I\, \Delta f\; Z_{DC}^2}{|\gamma\, l|^2} \tag{4.12}$$

and since

$$I\, Z_{DC} = V_{DC} \tag{4.13}$$

and

$$(\frac{V_{DC}}{l})(\frac{\mu}{l}) = \frac{v_d}{l} = \frac{1}{t_t} = \omega_c \tag{4.14}$$

this simplifies to

$$\overline{v_n^{\,2}} = 2\left(\frac{k\,T}{q}\right) q\,\Delta f\; Z_{DC}\left(\frac{\omega_c}{\omega}\right) \qquad (4.15)$$

at the surface of the sample for frequencies higher than the reciprocal transit time as shown in Figure 4.2.

These above results show 1/f noise due to fluctuations of charge and potential inside the high impedance semi-insulating material. The lowest radian frequency, $\omega_{\text{cth}}$, is just the reciprocal of the transit time in response to the thermal voltage, kT/q. Injecting current into high impedance semi-insulating materials with a large DC voltage drop across them will result in large mean square 1/f noise voltages.

The results are directly applicable to GaAs resistors on semi-insulating substrates [22]. The normal leakage current and at higher applied voltages impact ionization and multiplication of carriers in the drain region at higher drain voltages will result in non-trivial substrate currents being injected into the semi-insulating substrate. Large mean square 1/f noise voltages will result which will backgate the resistor channel and be amplified by the backgate transconductance of the device. This problem is of course very similar to the substrate current and backgate transconductance in MESFET's [23]-[24], except they are usually very short channel devices and operated in the saturation region which considerably complicates a detailed analysis.

### 4.3. Application The Theory of the 1/f Noise of Semi-Insulating Materials to GaAs Resistors

The device, GaAs resistor is in Cr-doped p-type semi-insulating substrate. The typical value of the doping concentration is of the order of $10^{17}$ $cm^{-3}$. The chromium introduces a unique deep acceptor level. Most of the Cr atoms are active in semi-insulating GaAs up to concentrations of the order of several $10^{17}$ $cm^{-3}$. Martin et al. [41] worked on compensation mechanisms in GaAs and showed Shockley diagram corresponding to a semi-insulating GaAs with a given concentration of the deep Cr acceptor and the deep donor EL2, with or without shallow donors. Figure 4.2 shows the diagram and Fermi level of semi-insulating GaAs. The figure shows the concentration of chromium, of the deep donor EL2, and shallow donors. The chromium concentration was determined from optical absorption measurements, but the concentration of EL2was approximated. The Fermi level is located between EL2 and Cr in Figure 4.3.

The 1/f noise phenomena associated with thin-filament resistor structure in GaAs such as shown in Figure 4.4, can now be calculated. The DC leakage and substrate current being injected into the semi-insulating substrate behind the GaAs filament produces backgate noise voltage as in equation (4.15);

$$\overline{v_n^2} = 2\left(\frac{kT}{q}\right) q\ \Delta f\ \ R\left(\frac{\omega_c}{\omega}\right) - - - - - V^2 \qquad (4.16)$$

where

$$R = \frac{d}{q\mu_p pWL} - - - - - \Omega \qquad (4.17)$$

where q is the carrier charge, k the Boltzman constant, T the temperature, R the low frequency DC resistance of the substrate behind the device, ω the radian frequency, $\omega_C = 1/t_t$ the reciprocal of the transit time of the carriers, d the thickness from the backgate contact to the depletion region, p the mobile charge in the substrate, $\mu_p$ the hole mobility in the semi-insulating substrate, and W and L are the width and length of the channel, respectively. The thickness of the semi insulating sample, d, is now the transmission line length, l. This backgate noise voltage is then amplified by the backgate transconductance, $g_{mbg}$.

$$\frac{\overline{i_n^2}}{\Delta f} = 2\left(\frac{kT}{q}\right) q\ R\ \frac{\omega_c}{\omega}\left(g_{mbg}\right)^2 \quad ----- A^2 / Hz \qquad (4.18)$$

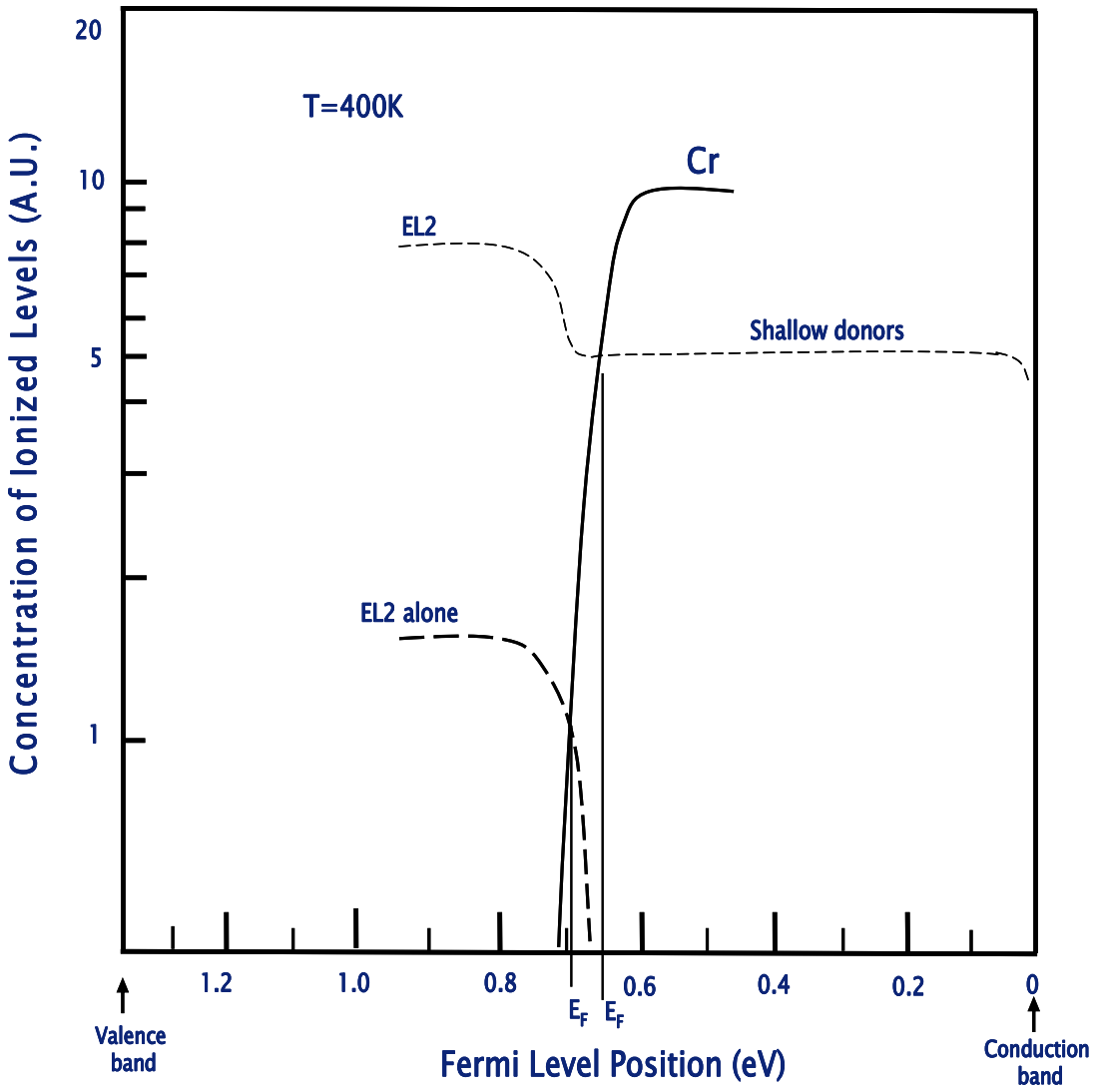


Figure 4.3 Shockley diagram corresponding to a semi-insulating GaAs. This figure is from Fig. 9 of Martin et al. [41].

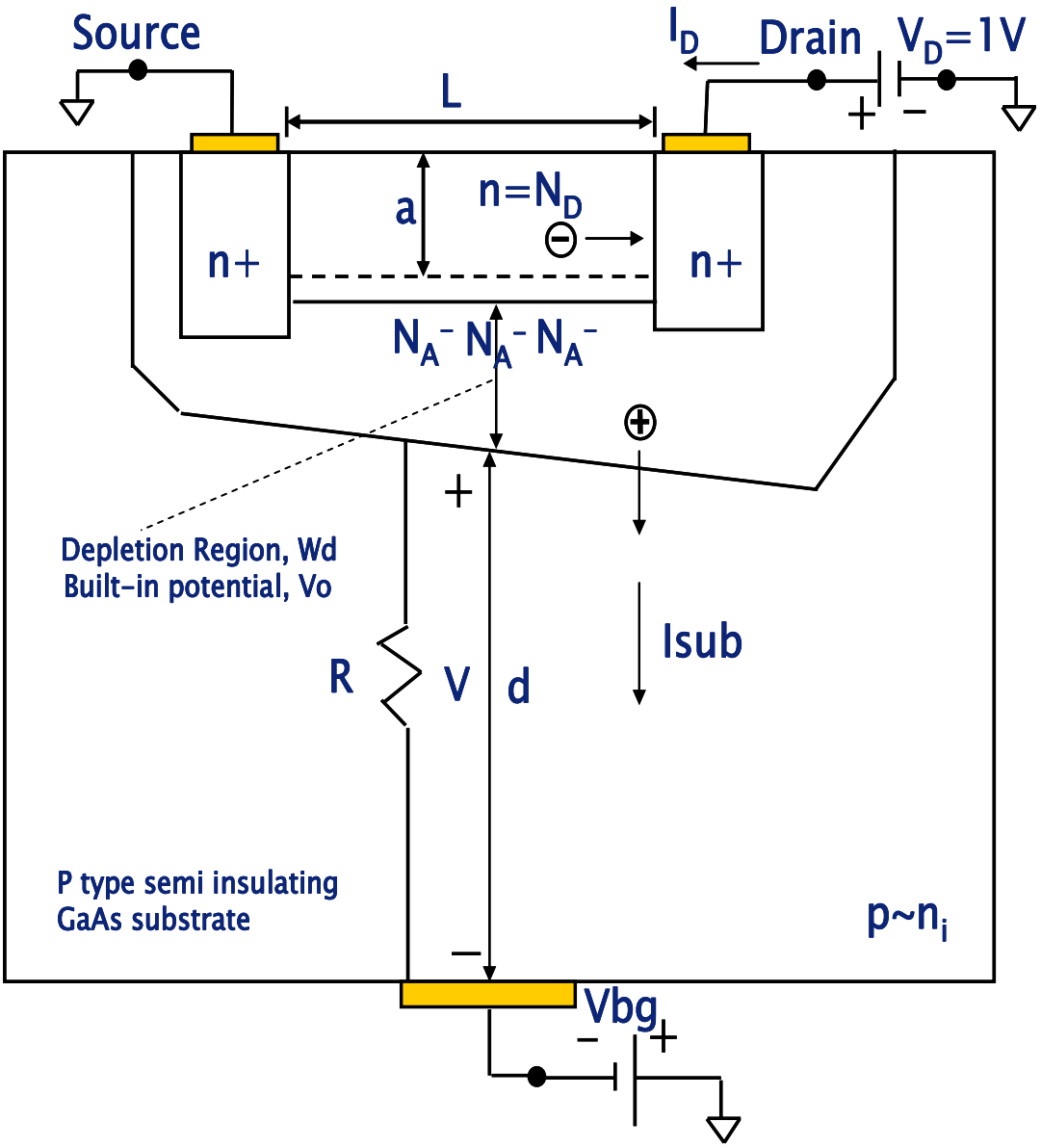


Figure 4.4 Cross-section of resistor device structure. The voltage, V develops across the substrate of thickness, d due to leakage and substrate current.

By applying small-signal backgate bias voltage, $V_{bg}$ to the semi-insulating substrate as shown in Figure 4.4, the variation of the depletion width, $W_d$ between n-channel and the semi-insulating GaAs can be found.

$$W_d = \sqrt{\frac{2\,\varepsilon_{GaAs}\,\varepsilon_o\left(V_0 + V_{bg}\right)}{q\,N_A}} \quad -----cm \tag{4.19}$$

where $\varepsilon_{GaAs}$ is the relative dielectric constant for GaAs, $\varepsilon_o$ the dielectric constant, and $V_o$ the built-in potential in the depletion region. The variation of charge in the channel,

$\Delta Q_{ch} = \Delta Q_{sub}$ is,

$$\Delta Q_{ch} \approx \frac{\partial W_d}{\partial V_{bg}}\,\Delta V_{bg}\; q\; N_A \quad -----Coul/cm^2 \tag{4.20}$$

and

$$\frac{\partial W_d}{\partial V_{bg}} = \frac{\varepsilon_{GaAs}\,\varepsilon_o}{q\,N_A\,W_d} \quad -----cm/V \tag{4.21}$$

In the linear operating region,

$$g_{mbg} = \frac{\partial I_d}{\partial V_{bg}} = \frac{\varepsilon_{GaAs}\,\varepsilon_o}{W_d\,Q_{ch}}\,I_D \quad -----S \tag{4.22}$$

$$g_{mbg} = \frac{\varepsilon_{GaAs}\,\varepsilon_o}{W_d}\,\mu_n\,V_D\,\frac{W}{L} \quad -----S \tag{4.23}$$

where $I_D$ is the drain current, $V_D$ the bias voltage at the drain, and $\mu_n$ the electron mobility.

This backgate transconductance, $g_{mbg}$ predicts the very high 1/f corner frequencies being observed [22] when the thermal noise is equated to the 1/f noise given by equation (4.18) as shown in Figure 4.5;

$$\omega_{1/f} = \frac{g_{mbg}}{2\, g_d}\left(g_{mbg}\ R\right)\omega_c \ \ -----rad/\sec \tag{4.24}$$

where $g_d$ is the drain conductance, or conductance of the resistive filament. The thermal mean square noise current spectrum is

$$\frac{\overline{i_n^2}}{\Delta f} = 4\left(\frac{kT}{q}\right) q\ g_d \ \ -----A^2\ /\ Hz \tag{4.25}$$

and

$$g_{mbg}\left(g_{mbg}\ R\right) = \left(\frac{\varepsilon_{GaAs}\varepsilon_o}{W_d}\mu_n V_D \frac{W}{L}\right)^2 \frac{d}{q\mu_p pWL} -----S \tag{4.26}$$

$$g_{mbg}\left(g_{mbg}\ R\right) = \frac{\varepsilon_{GaAs}\varepsilon_o \mu_n^2 W d}{2L^3 \mu_p}\frac{V_D^2}{\left(V_o + V_{bg}\right)}\frac{N_A}{p} -----S \tag{4.27}$$

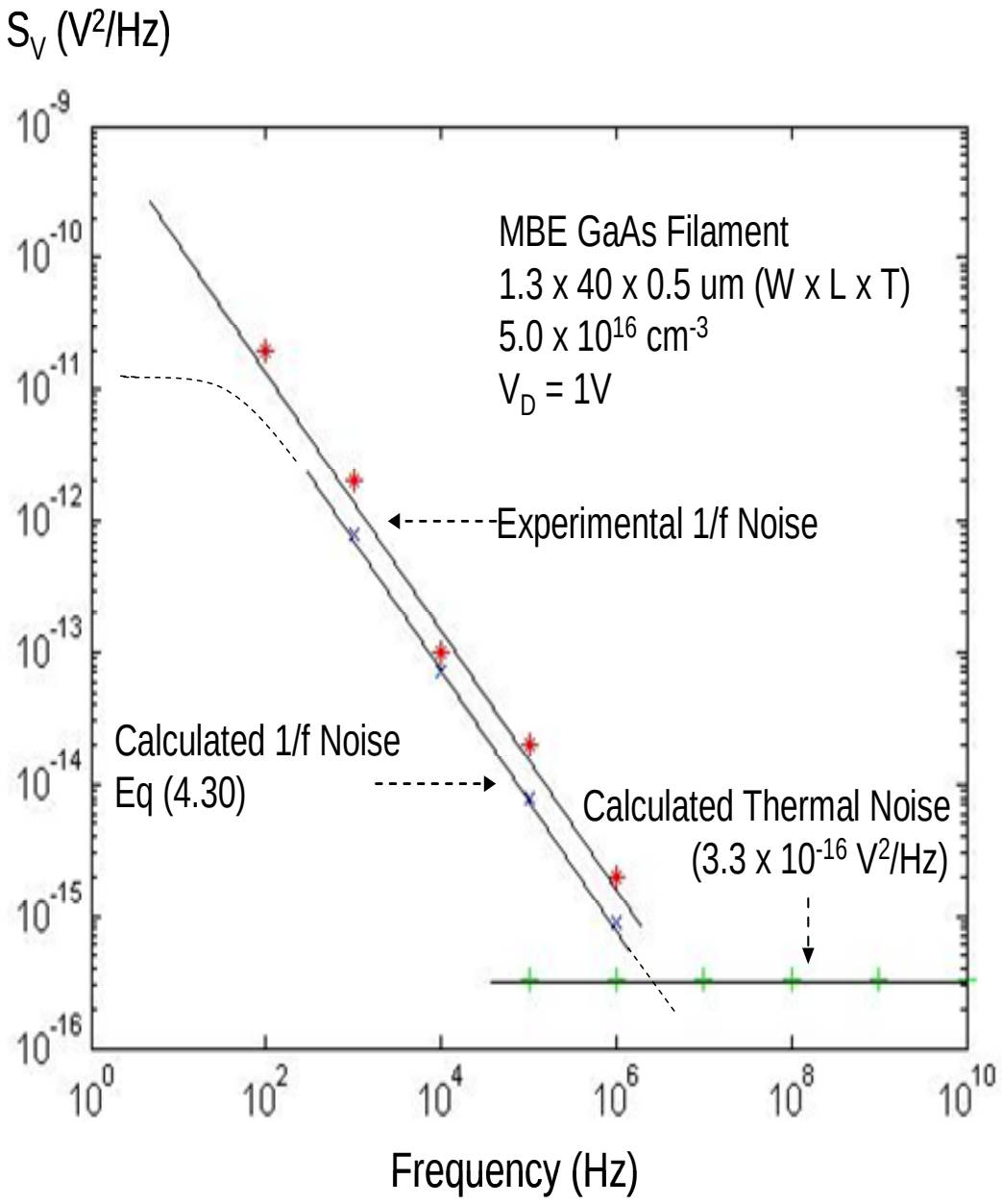


Figure 4.5 Mean square noise voltage spectrum of GaAs resistor. Experimental data are from Fig. 3 of Tacano and Sugiyama [22].

The results of equation (4.18) can be explained in terms of Hooge's fundamental relationship $S_V=\alpha_H V^2/fN$ where V is the voltage across the device, f and N are the frequency and the total number of carriers, respectively, and where $\alpha_H$ is Hooge's noise parameter originally determined as $\alpha_H = 2.0 \times 10^{-3}$ [25], [26].

Hooge's noise parameter can be expressed in terms of the device parameters by using equations (4.16) and (4.23).

$$\overline{v_{nd}^2} = \frac{\overline{i_n^2}}{g_d^2} = \overline{v_n^2}\left(\frac{g_{mbg}}{g_d}\right)^2 \quad -----V^2 \tag{4.28}$$

$$\left(\frac{g_{mbg}}{g_d}\right)^2 = \frac{1}{2}\frac{\varepsilon_{GaAs}\,\varepsilon_o}{q\,a^2}\frac{N_A}{N_D^2}\frac{V_D^2}{\left(V_o + V_{bg}\right)} \tag{4.29}$$

where a is the thickness of the channel, and $V_o$ the built-in potential in the depletion region.

From equations (4.28), and (4.29), the noise voltage spectrum at the drain is then

$$\begin{aligned}\frac{\overline{v_{nd}^2}}{\Delta f} &= \alpha_H \frac{V_D^2}{N f} \\ &= \frac{1}{2\pi}\left(\frac{kT}{q}\right)\frac{1}{f}\frac{V_D^2}{qaN_D}\frac{\varepsilon_{GaAs}\varepsilon_o}{WLd}\frac{V}{(V_o - V)}\frac{1}{aN_D}\frac{N_A}{p} \quad ---V^2/Hz\end{aligned} \tag{4.30}$$

where $N=aN_DWL$, V is the voltage across the semi-insulating substrate, $V=-V_{bg}$, $p=\sim n_i$, $V_0$ is much larger than V, then

$$\alpha_H = \frac{1}{2\pi}\left(\frac{kT}{q}\right)\frac{C_{sub}}{Q_{ch}}\frac{V}{(V_o - V)}\frac{N_A}{p} \tag{4.31}$$

where $C_{sub}=\varepsilon_{GaAs}\varepsilon_o/d$ is the substrate capacitance.

**4.4. Comparison to Published Data**

Figure 4.5 shows the experimental results of M. Tacano and Y. Sugiyama [22] for a 1.3um x 40um x 0.5um (width x length x thickness) GaAs filament resistor. Equation (4.30) gives the noise voltage spectral density $S_v(f) = \overline{v_{nd}^2} / \Delta f$, and has been evaluated at $V_D$=1V using the parameters in Figure 4.5 and assuming d=5x$10^{-2}$ cm to give the calculated line in Figure 4.5. In equation (4.30) we used V=5.7 x $10^{-6}$V, T=300 K, p = $n_i$ exp[($E_i$-$E_F$)/kT] ~ $n_i$ = 1.0x$10^8$ $cm^{-3}$, $N_A$=1.0 x$10^{17}$ $cm^{-3}$, and $\varepsilon_{GaAs}$= 13.2. However, p can be probably much greater than $n_i$, then V> 2kT/q ~ 50mV. The calculated resistance of the substrate under the device is 9.62 x $10^{11}$ Ohm. The current through the semi insulating substrate is 5.93x$10^{-18}$ A.

The noise spectrum of a GaAs resistor of one particular device dimension taken from the published literature [22] is plotted as a function of the applied voltage and is shown in Figure 4.6. It is evident that noise level increases in proportion to the square of the terminal voltage at moderate drain bias [22]. These experimental results can be explained at moderate bias conditions by the equations (4.16), (4.23), and (4.30).

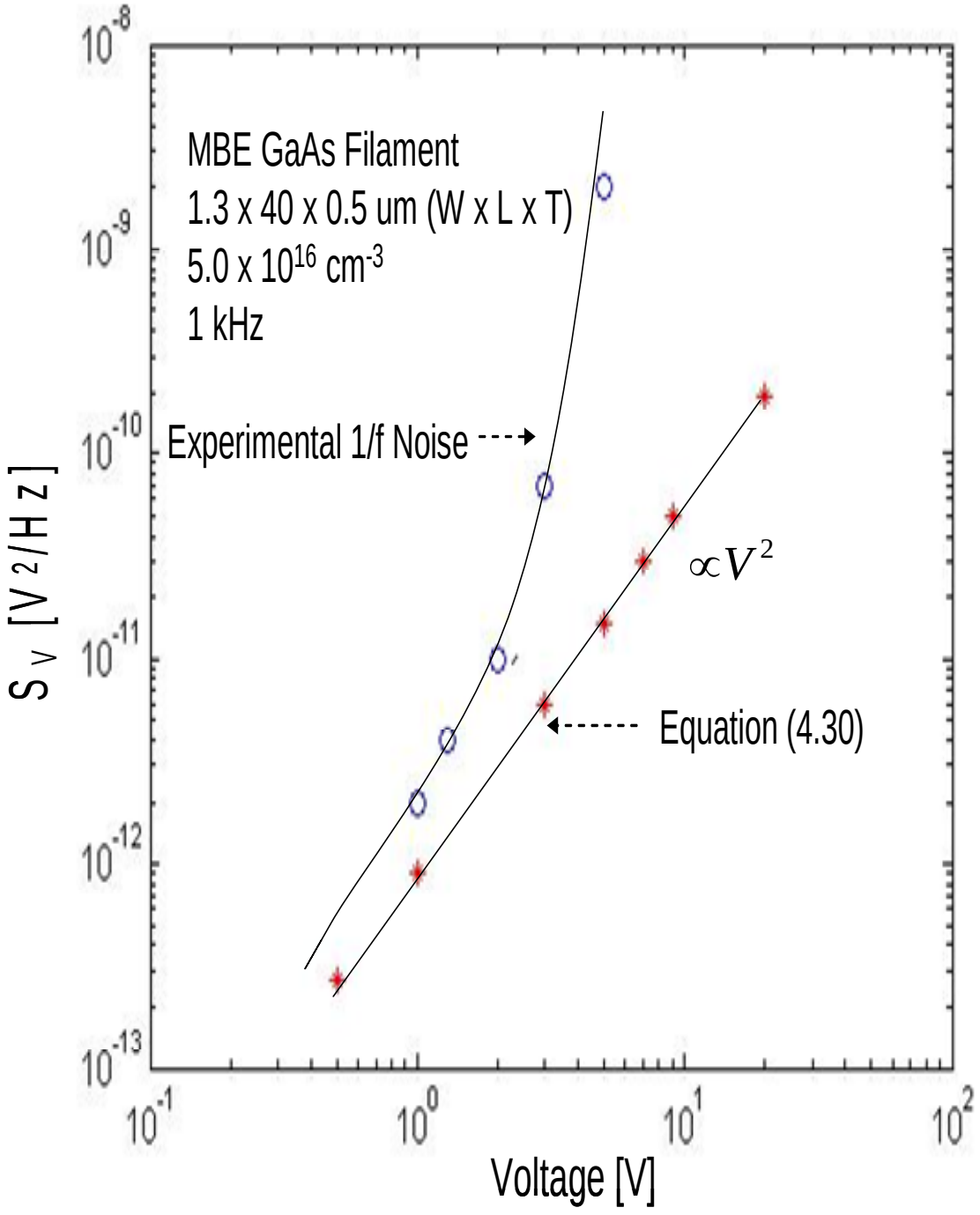


Figure 4.6 Dependence of noise voltage on drain bias. Experimental data are from Fig.6 of Tacano and Sugiyama [22].

We here also calculated, by using equations (4.24), (4.27), and (4.32) as shown below, the 1/f corner frequency of this n-GaAs filament with an applied voltage $V_D$ =1.0V.

$$\omega_{1/f} = \frac{\varepsilon_{GaAs}\varepsilon_o \mu_n V_D^2}{4qN_D L^2 ad} \frac{V}{(V_o - V)} \frac{N_A}{p} - - - - - rad/\sec \qquad (4.32)$$

The value of the 1/f corner frequency of the above device is 3.49 x $10^6$ Hz which is shown in Figure 4.5.

We have assumed here that although the devices are two terminal devices that they are mounted in a package cavity and that the back plane of the cavity is grounded. The description of the experiments [22] is not clear in this regard. If there is no back contact or substrate contact then the substrate current must forward bias the source substrate junction and all leakage currents flow out through the source. This will not change the nature of the results but makes the geometrical interpretation more complex. We have done similar measurements on MESFET's where the substrate is grounded [23], [24]. In the next section, we will present our own measurements on commercially available GaAs resistors showing that the lack of a substrate contact changes the results slightly but not the conclusions, a two terminal device does not lend itself to a simple analysis. It is also evident that (4.30) can predict the dependence of noise on drain voltage squared as shown in Figure 4.6.

Hooge's noise parameter in equation (4.31) has been calculated and agrees quite well with the experimental values for low electric fields. The calculated value of the noise parameter is 2.0 x $10^{-3}$ at T= 300 K. The increase in Hooge's parameter at higher bias conditions and electric fields can be explained by (4.31)

which also shows explicitly a considerable increase in this noise parameter and the corresponding noise level with high electric fields. This model seems to fit the published experimental data in [38] at least as well if not better than the quantum 1/f noise model.

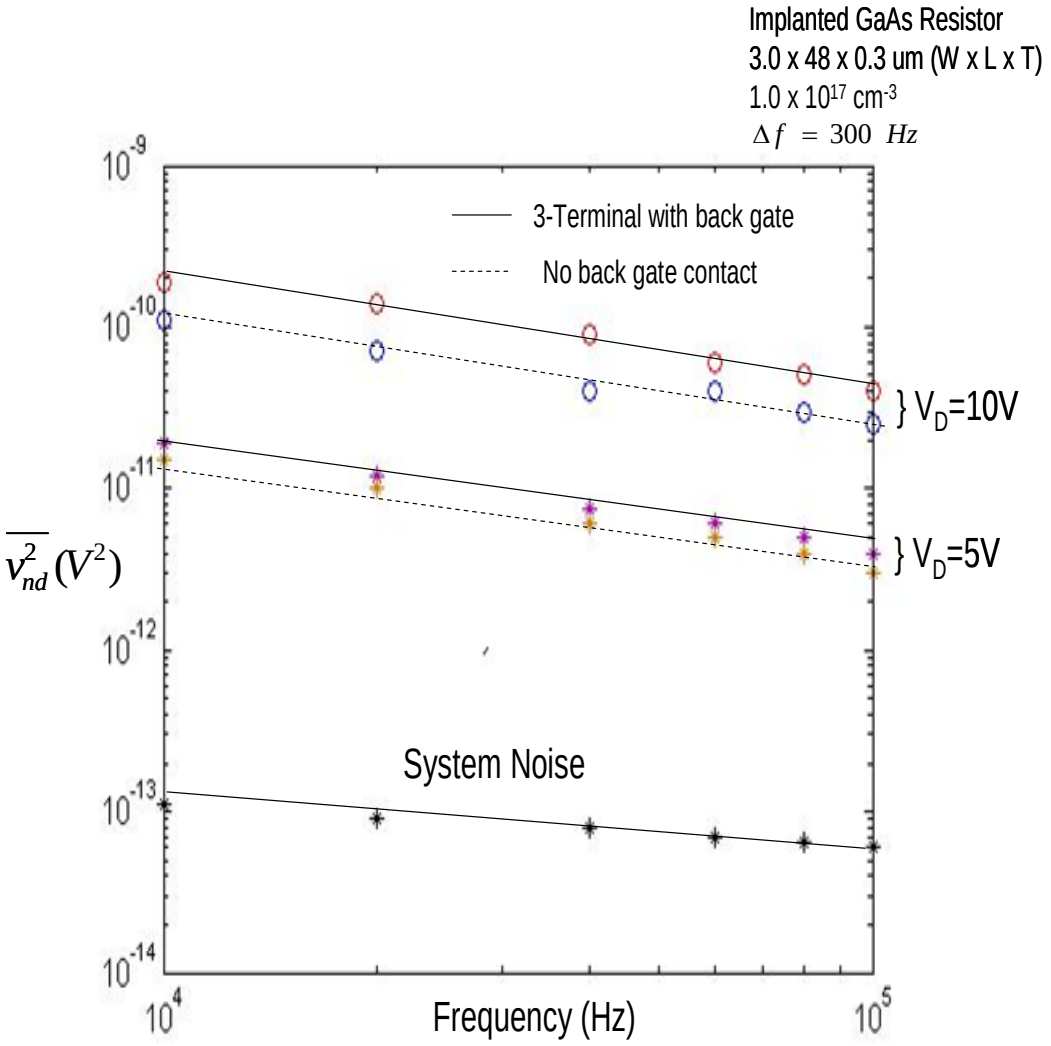


Figure 4.7 Measured mean square noise voltage of a GaAs resistor, with and without backgate contact.

**4.5. Comparison to Our Experimental Results**

Given that in the published data on GaAs filaments [22] or resistors it is not clear whether the devices have a substrate contact, are three terminal devices, or do not have a substrate contact, are two terminal devices; then we have made our own measurements on implanted GaAs resistors. It is possible then to measure these devices both with and without substrate connections as has been done and as is shown in Figure4.7.

The resistors are just gateless FET channel implants and a normal component in a commercially available foundry service process available from TriQuint Semiconductor, Beaverton, Oregon. The particular devices we have characterized have a normal resistance of $10^4$ ohms at room temperature. The mean square noise voltage has been measured using a low noise bipolar transimpedance amplifier and Tektronix spectrum analyzer. The spectral intensity as shown in Figure 4.7 is,

$$S_v(f) = \frac{\overline{v_n^2}}{\Delta f} = \frac{\alpha_H V_D^2}{N f}$$

Using the previous definitions then

$$\alpha_H = \frac{1}{2\pi}\left(\frac{kT}{q}\right)\frac{C_{sub}}{Q_{ch}}\frac{V}{(V_o - V)}\frac{N_A}{p}$$

where $C_{sub}$ (F/cm$^2$) is the capacitance of the substrate under the resistor and $Q_{ch}$ is the implanted charge in the channel ($Q_{ch}/q \sim 3 \times 10^{12}$ cm$^{-2}$). Hooge's parameter has a very simple interpretation. $C_{sub}(kT/q)$ is the charge developed by the thermal voltage (kT/q) across the substrate capacitance, and $Q_{ch}$ is the implanted charge in the channel. Hooge's parameter is no parameter, but rather is

given by a formula which simply relates the ratio of these two charges with proportional constant which depends on the voltage developed in the semi-insulating substrate and doping concentration of the substrate.

**4.6. Discussions**

We have studied the 1/f noise of resistive filaments in n-GaAs and compared this to published data and our own experimental data. The equations derived predict as observed that the noise level increases in proportion to the square of the terminal voltage. We have derived equations to calculate the product $g_{mbg}^2 R$ and to predict the 1/f corner frequency, the corner frequency calculated corresponds well with that observed in published experimental results. The increase in Hooge's noise parameter with an increase in the voltage drop in the semi-insulating substrate at high electric fields is also predicted. Hooge's parameter in this particular case, is in reality no parameter, but is given by a formula which simply relates the ratio of the charge developed by thermal voltage across the capacitance of the substrate and the implanted charge in the channel with proportional constant which depends on the voltage developed in the semi-insulating substrate and doping concentration of the substrate.

These concepts are probably also applicable to other 1/f noise phenomena which occur in nature, and there may in reality be many analogs in nature. Basically, the concept is that any natural system of large extent, high resistance and some capacity when disturbed will respond by generating 1/f noise, due to their distributed nature.

# 5. 1/f NOISE DUE TO TEMPERATURE FLUCTUATIONS IN HEAT CONDUCTION IN BIPOLAR TRANSISTORS

## 5.1. Introduction

We have previously shown that any system having a large capacity or capacitance, large extent and high resistance will respond when disturbed by generating 1/f noise [18]. This has been demonstrated by finding the frequency dependent solutions to the diffusion equation using equivalent circuit techniques [14] [15]. The R-C transmission line which results has been used to describe charge and potential fluctuations in semi-insulating materials [18], the 1/f noise of FETs on semi-insulating substrates [42-44] [24] and the 1/f noise of GaAs resistors on semi-insulating substrates [45]. This type of transmission line is in reality of course a diffusion line.

Another more direct example perhaps is heat conduction itself described by the diffusion equation where many materials have a large heat capacity, high thermal resistance, and significant distances to a heat sink. As a consequence 1/f noise should be expected and is observed in heat conduction [46]. Bipolar transistors operating at large power dissipation should be a good example and will be shown here to be so, significant heat conduction occurs over finite distances with appreciable diffusion transit times. The temperature of the transistor is only an average value and there are fluctuations about this average value which can have a 1/f frequency dependence, these temperature fluctuations modulate the base-emitter junction characteristics and result in a mean square collector noise current [46].

The concept of temperature fluctuations about a steady state nonequilibrium value is not only expected but in itself not new. A textbook formulation of the problem of frequency dependent solutions to the diffusion equation has been given by Kittel and Kroemer [47], where they note that high frequency variations will be strongly attenuated. The problem of noise in resistors due to temperature fluctuations due to heat conduction through a substrate has been treated by van der Ziel et al. [48], where they obtained a more or less 1/f dependence. More recently, the problem of temperature fluctuations in heat conduction has been analyzed in the framework of fluctuating hydrodynamics [49] [50]. What is new here is our treatment of this problem by transmission line techniques and application to electron devices [46].

## 5.2. The Theory of 1/f Noise Due to Temperature Fluctuations in Heat Conduction

The R-C transmission lines previously analyzed [18] are in reality diffusion lines and potential and currents are described by the diffusion equation;

$$\frac{\partial^2 V}{\partial x^2} = R\,C\,\frac{\partial V}{\partial t} \tag{5.1}$$

This is the same type of equation describing heat conduction [47];

$$a\,\frac{\partial^2 T}{\partial x^2} = \frac{\partial T}{\partial t} \tag{5.2}$$

where a is the thermal diffusivity, $m^2$/sec in MKS units and T is the temperature. An equivalent circuit representation can also be made for heat conduction as shown in Figure 5.1 and 5.2 where for each volume element,

$$R = \frac{1}{KA} \qquad [K/W \cdot m] \tag{5.3}$$

$$C = C_p \rho A \qquad [J/K \cdot m] \tag{5.4}$$

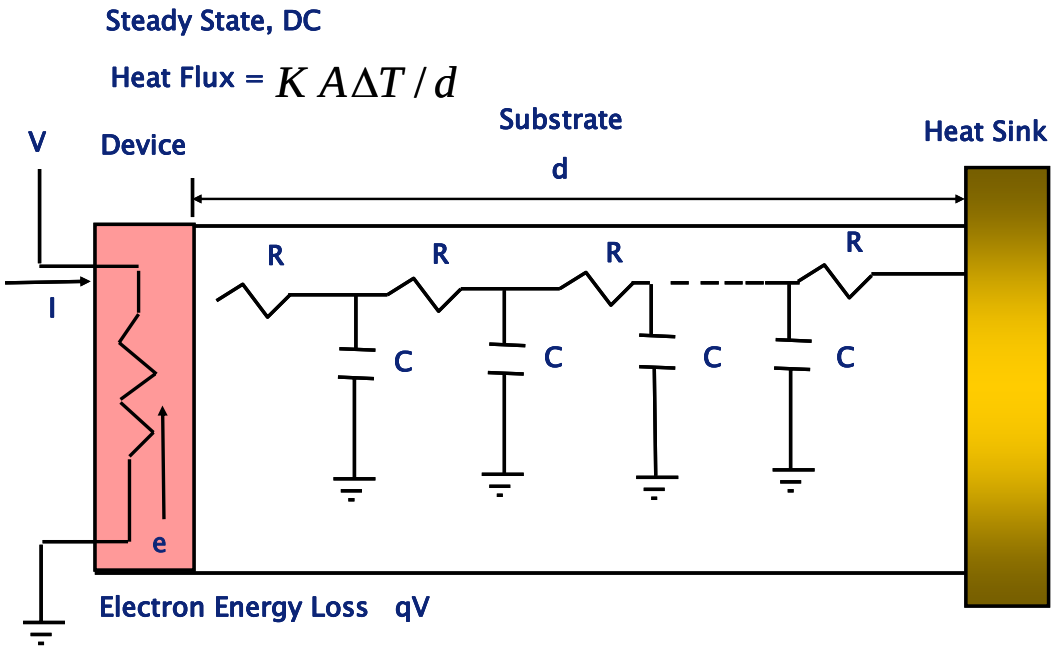


Figure 5.1 Steady state heat conduction model due to power dissipation in a resistor.

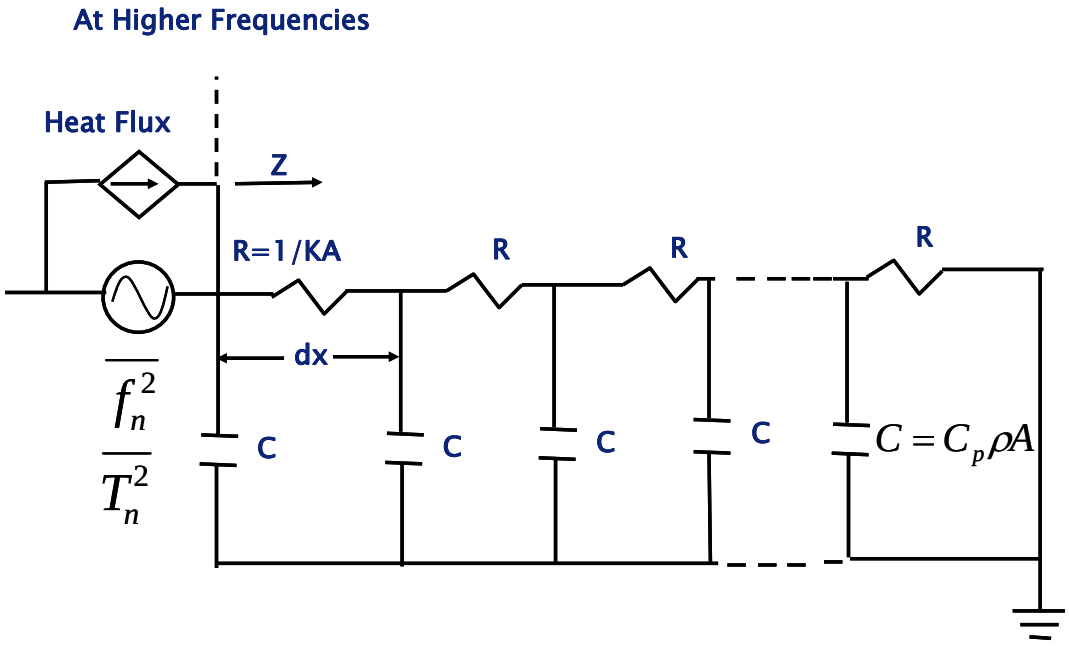


Figure 5.2 The transmission line model showing the resistance and capacitance associated with heat conduction in the bulk of the sample.

where K is the thermal conductivity, $C_p$ the heat capacity, $\rho$ the density, and A the area of the sample through which there is heat conduction. The thermal conductivity K of a material is the rate of transfer of heat per unit time, per unit cross-sectional area, per unit temperature gradient. The heat capacity $C_p$ is the amount of heat required to raise the temperature of an unspecified mass by one degree of temperature. Temperature is analogous to voltage and heat flux analogous to current.

The time invariant steady state, or DC, solution for this line is governed by the Fourier equation, which in one-dimensional form is expressible as

$$F = \mathrm{K}A\frac{dT}{dx} \qquad [\mathrm{W}] \qquad (5.5)$$

where F is the heat flux, and dT/dx is the temperature gradient in the direction of heat flow.

The total line flux is

$$flux = \mathrm{K}\, A \frac{\Delta T}{d}. \qquad (5.6)$$

The temperature difference resulting from the steady-state diffusion of heat is thus related to the thermal conductivity of the material, the cross-sectional area, and the path length, d (Figure 5.3), according to

$$(T_1 - T_2) = flux \cdot \frac{d}{KA}\ . \qquad [\mathrm{K}] \qquad (5.7)$$

The form of the above equation suggests that the thermal resistance of the entire structure is given by

$$R_{DC} = \frac{(T_1 - T_2)}{flux} = \frac{d}{KA}. \qquad [\mathrm{K/W}] \qquad (5.8)$$

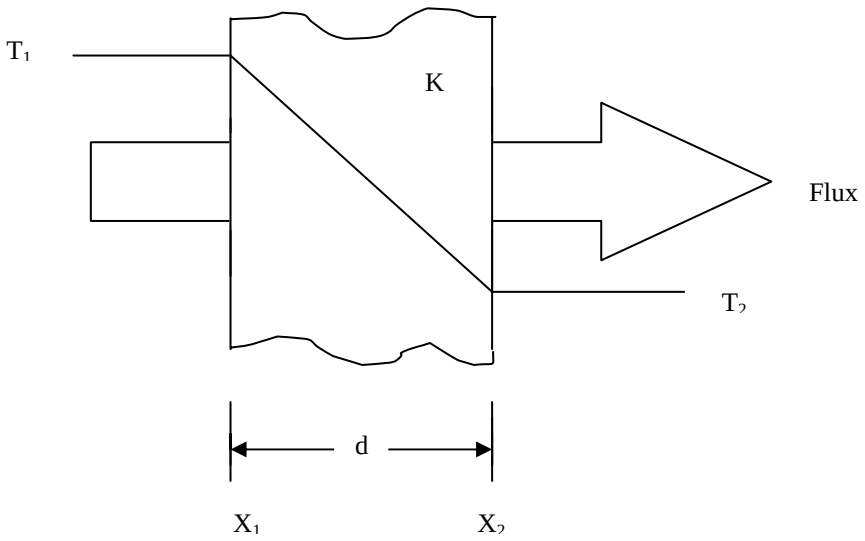


Figure 5.3 Heat transfer by conduction through material.

The thermal conductivity and diffusivity are not independent but are related in a form which we will later find useful,

$$\frac{a}{\mathrm{K}} = \frac{1}{C_p\ \rho} \qquad \frac{K \cdot m^3}{J} \tag{5.9}$$

The steady state time dependent solutions of this differential equation and transmission line , of length l=d, in response to a sinusoidal excitation in temperature T at the sending end of this line are described by the AC impedance looking into this line, $Z_s$ .

At very low frequencies, however, the sending end impedance is just

$$Z_s = Z_o \tanh \gamma\ l \approx Z_o\ \gamma\ l \tag{5.10}$$

but this is just $R_{DC}$. At high frequencies this line is strongly attenuating [47] and the impedance looking into this long lossy line is just $Z_o$, but

$$Z_o = \frac{R_{DC}}{\gamma l} \tag{5.11}$$

where

$$\gamma = \sqrt{Z\ Y} = \sqrt{R\ j\omega\ C} \tag{5.12}$$

but RC = 1/a from equations (5.1) and (5.2)

and then

$$\gamma = \sqrt{\frac{j\omega}{a}}\ . \tag{5.13}$$

Thus we can find simple solutions for the two limiting cases, DC and high AC frequencies.

$$Z_s\ (DC) = R_{DC} \tag{5.14}$$

$$Z_s\ (High\ Frequency\ AC) = Z_o = \frac{R_{DC}}{\gamma\, l} \tag{5.15}$$

where

$$\gamma\, l = \sqrt{j\,\omega\,\frac{l^2}{a}} \tag{5.16}$$

$$\left|\gamma\, l\right|^2 = \omega\, l^2\ /\ a \tag{5.17}$$

and then

$$\left|Z_s\right|^2 = R_{DC}^2\ /\left|\gamma\ l\right|^2\ . \tag{5.18}$$

If we now let $\omega_{cth} = a\ /\ l^2$, which is one half of $2\ a\ /\ l^2$ or the reciprocal of the diffusion transit time, then,

$$\left|Z_s\right|^2 = \frac{R_{DC}^2\ \omega_{cth}}{\omega} = \frac{R_{DC}^2\ a}{l^2\ \omega} \tag{5.19}$$

$$\left|Z_s\right|^2 = \frac{d^2}{\left(\mathrm{K}\ A\right)^2}\ \frac{a}{d^2}\ \frac{1}{\omega}\,. \tag{5.20}$$

### 5.3. Non-equilibrium Case with Heat Conduction

As is the case with electrical current, which is made up of a large number of individual events, heat flux is associated with the transfer of energy to lattice vibrations in discrete elements. We will assume here, as shown in Figure 5.1, that the heat energy is transferred to the lattice over very short time periods in the units of $V_{DC}$ q where $V_{DC}$ is the applied DC voltage. We are assuming here that the transit time of the electron through the electron device is small, as is usually the case. Using Carson's theorem then,

$$S_f(f) = 2\overline{N}\left|f(\omega)\right|^2 \tag{5.21}$$

in which each individual event occurs in a short time then

$$S_f(f) = 2\overline{N}V_{DC}^2 q^2 \tag{5.22}$$

But the heat flux is just the mean number of individual units of energy times the energy associated with each, $flux = \overline{N}\ q\ V_{DC}$, which means the spectral intensity of the heat flux becomes, as shown in Figure 5.2

$$S_f(f) = 2qV_{DC}\ flux = \overline{f_n^2}/\Delta f \tag{5.23}$$

This spectral intensity will cause a mean square temperature variation with spectral intensity at the surface of the sample given, as shown in Figure 5.2, by

$$S_T(f) = \overline{T_n^2}/\Delta f = \overline{f_n^2}\left|Z_s\right|^2/\Delta f \tag{5.24}$$

Again the solution is simple in the two limiting cases; at low frequencies or DC then

$$S_T(f) = \overline{T_n^2}/\Delta f\ = 2qV_{DC}\ flux\left(\frac{d}{\mathrm{K}A}\right)^2 = 2qV_{DC}\overline{N}qV_{DC}\frac{d}{\mathrm{K}A}\frac{d}{\mathrm{K}A} \tag{5.25}$$

$$S_T(f) = \overline{T_n^2}/\Delta f\ = 2qV_{DC}\Delta T\frac{d}{\mathrm{K}A} \tag{5.26}$$

while at high frequencies;

$$S_T(f) = \overline{T_n^2}/\Delta f\ = 2qV_{DC}\ flux\left|Z_s\right|^2 \tag{5.27}$$

$$= 2qV_{DC}\overline{N}qV_{DC}\frac{d}{\mathrm{K}A}\frac{d}{\mathrm{K}A}\frac{a}{d^2\omega} \tag{5.28}$$

$$S_T(f) = 2qV_{DC}\Delta T\left(\frac{a}{\mathrm{K}Ad}\right)\frac{1}{\omega}\ (K)^2\cdot\sec \tag{5.29}$$

but $a/(\mathrm{K}\,A\,d)$ can be simplified by using $a/\mathrm{K}=1/(C_p\,\rho)$ and is just the reciprocal of the total heat capacity of the sample

$$\frac{a}{\mathrm{K}\,A\,d}=\frac{1}{C_p\ \rho\ Ad} \qquad \text{K/J} \tag{5.30}$$

The spectrum density of temperature fluctuation can also be written as

$$S_T(f)=\frac{1}{N}(\Delta T)^2\frac{2a}{d^2}\frac{1}{\omega} \tag{5.31}$$

## 5.4. Application of the Theory of 1/f Noise Due to Temperature Fluctuations to Resistors

Consider the example of heating a resistive filament and using equation (5.26) at low frequencies yields

$$S_T(f)=\overline{T_n^2}/\Delta f\ =2qV_{DC}\Delta T\frac{d}{\mathrm{K}\,A}\ \text{at low frequencies} \tag{5.32}$$

but the heat flux is

$$flux=\mathrm{K}\,A\frac{\Delta T}{d},or\frac{d}{KA}=\frac{\Delta T}{V_{DC}I_{DC}} \tag{5.33}$$

which yields

$$S_T(f)=\overline{T_n^2}/\Delta f\ =2q\frac{\Delta T^2}{I_{DC}} \qquad \text{K}^2\text{.sec} \tag{5.34}$$

if the resistance varies linearly with temperature

$$R\propto T \tag{5.35}$$

$$\frac{\overline{V_n^2}}{\Delta f}=\frac{\overline{T_n^2}}{T^2\Delta f}V_{DC}^2 \tag{5.36}$$

but then,

$$\frac{\overline{v_n^2}}{\Delta f} = 2qI\left(\frac{\Delta T}{T}\right)^2\left(\frac{V_{DC}}{I}\right)^2 \tag{5.37}$$

and

$$\frac{\overline{i_n^2}}{\Delta f} = 2qI\left(\frac{\Delta T}{T}\right)^2 \qquad \text{A}^2.\text{sec} \tag{5.38}$$

note that if $\Delta T = T$, then we just get the shot noise formula

$$\frac{\overline{i_n^2}}{\Delta f} = 2qI \quad \text{A}^2.\text{sec.} \tag{5.39}$$

In most instances, except filaments in vacuum, $\Delta T << T$. For resistive filaments in vacuum the spectral intensity at low frequency is

$$\frac{\overline{i_n^2}}{\Delta f} = 2qI\left(\frac{\Delta T}{T}\right)^2 \tag{5.40}$$

and $\Delta T >> T$. For high frequencies this varies as 1/f and using (5.31) instead of (5.26) above yields

$$\frac{\overline{v_n^2}}{\Delta f} = \frac{1}{N}\left(\frac{\Delta T}{T}\right)^2\left(\frac{2\,a}{d^2\omega}\right)V_{DC}^2 \tag{5.41}$$

$$\frac{\overline{v_n^2}}{\Delta f} = 2qI\left(\frac{\Delta T}{T}\right)^2\left(\frac{a}{d^2\omega}\right)\left(\frac{V_{DC}}{I}\right)^2 \tag{5.42}$$

and

$$\frac{\overline{i_n^2}}{\Delta f} = 2qI\left(\frac{\Delta T}{T}\right)^2\left(\frac{a}{d^2\omega}\right) \tag{5.43}$$

## 5.5. Application of the Theory of 1/f Noise Due to Temperature Fluctuations to Diodes and Transistors

Diodes operating under large bias currents can be expected to have significant power dissipation and heat conduction to the heat sink. This heat conduction will result in a temperature fluctuation and consequently 1/f electrical noise.

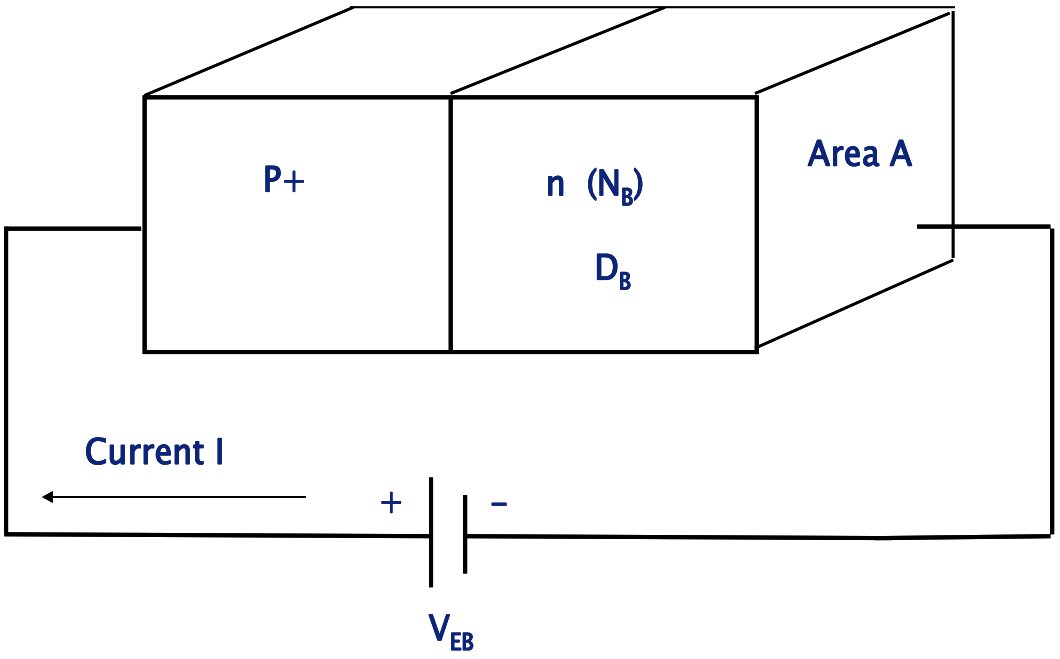


Figure 5.4 Forward biased diode with current depends on temperature variation.

Figure 5.4 illustrates a diode forward biased with current. The current in diode can be represented by this equation

$$I_C \cong qAn_i^2 \frac{D_B}{WN_B} \exp\left(\frac{qV_{EB}}{kT}\right) \tag{5.44}$$

where A is area, $D_B$ is diffusion constant in the base, W is base width, $N_B$ is the base doping concentration, and $V_{EB}$ is the dc bias across the p-n junction. The intrinsic carrier concentration depends on temperature because thermal energy is the source of carrier excitation across the forbidden energy gap. The intrinsic concentration is also a function of the size of the energy gap since fewer electrons can be excited across a larger gap. We shall be able to show that under most conditions $n_i^2$ is given by the expression

$$n_i^2 = N_c N_v \exp\left(\frac{-E_g}{kT}\right) \tag{5.45}$$

where $N_c$ and $N_v$ are related to the density of allowed states near the edges of the conduction band and valence band, respectively.

Thus the diode current equation (5.44) can be represented by

$$I_c = qA\frac{D_B}{WN_B}N_c N_v \exp\left(\frac{-E_g}{kT}\right)\exp\left(\frac{qV_{EB}}{kT}\right) \quad . \tag{5.46}$$

And we will assume this equation as

$$I = B\exp\left(\frac{-E_g}{kT}\right)\exp\left(\frac{qV_{DC}}{kT}\right) \tag{5.47}$$

where $V_{DC}$ is the bias voltage, B is a constant which depends only on the power laws of temperature, $E_g$ is the bandgap energy, and I is the diode current. Note that the forward bias voltage is a linearly decreasing function of temperature. Figure 5.5 illustrates a diode forward biased with a constant current. From the above equation (5.47) the bias voltage is

$$V_{DC} = \frac{E_g}{q} + \frac{kT}{q}\ln\left(\frac{I}{B}\right) \tag{5.48}$$

and

$$\Delta V = \left( -\frac{E_g}{q} + V_{DC} \right) = \frac{kT}{q} \ln\left( \frac{I}{B} \right) \tag{5.49}$$

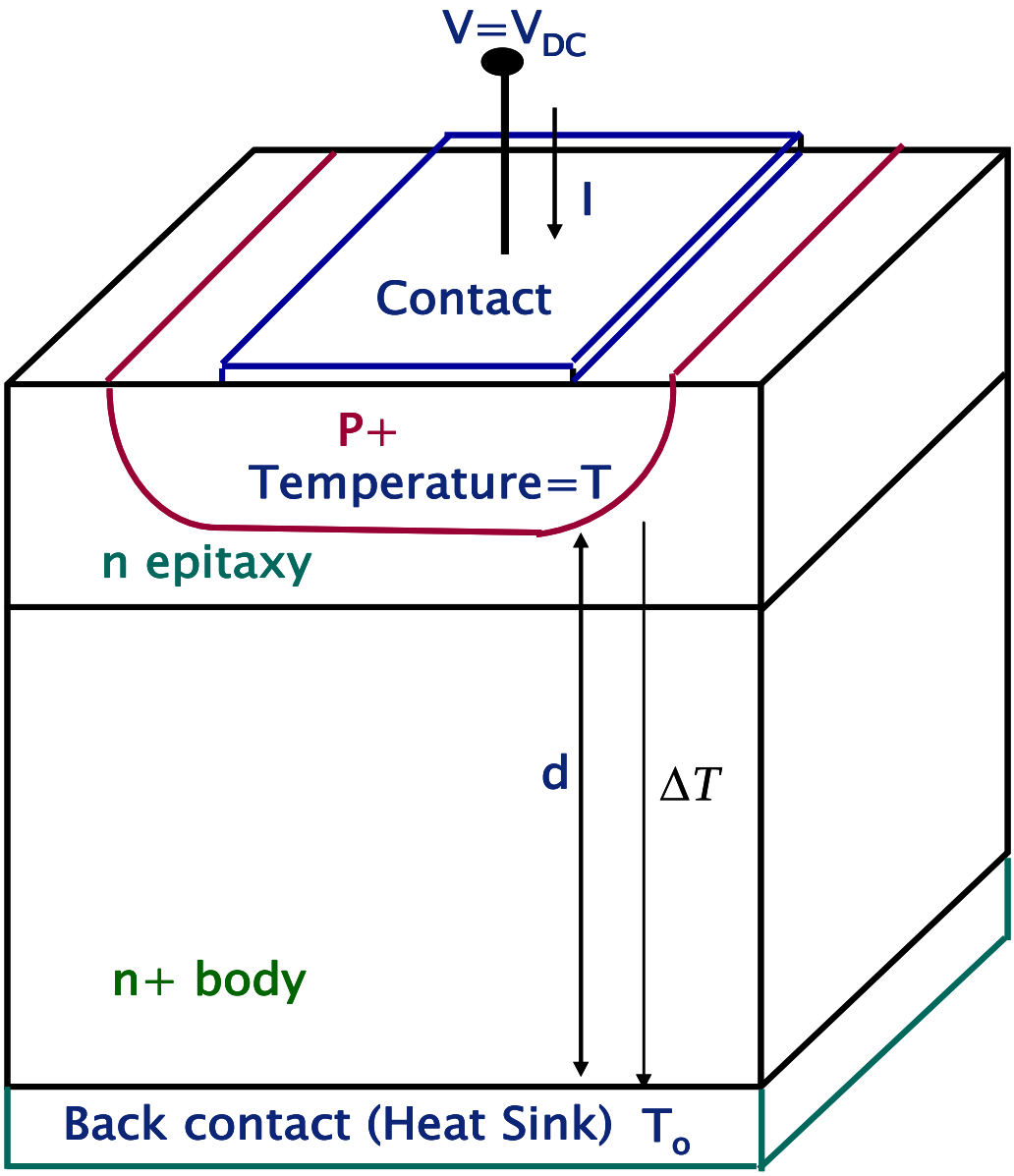


Figure 5.5 Diode cross section.

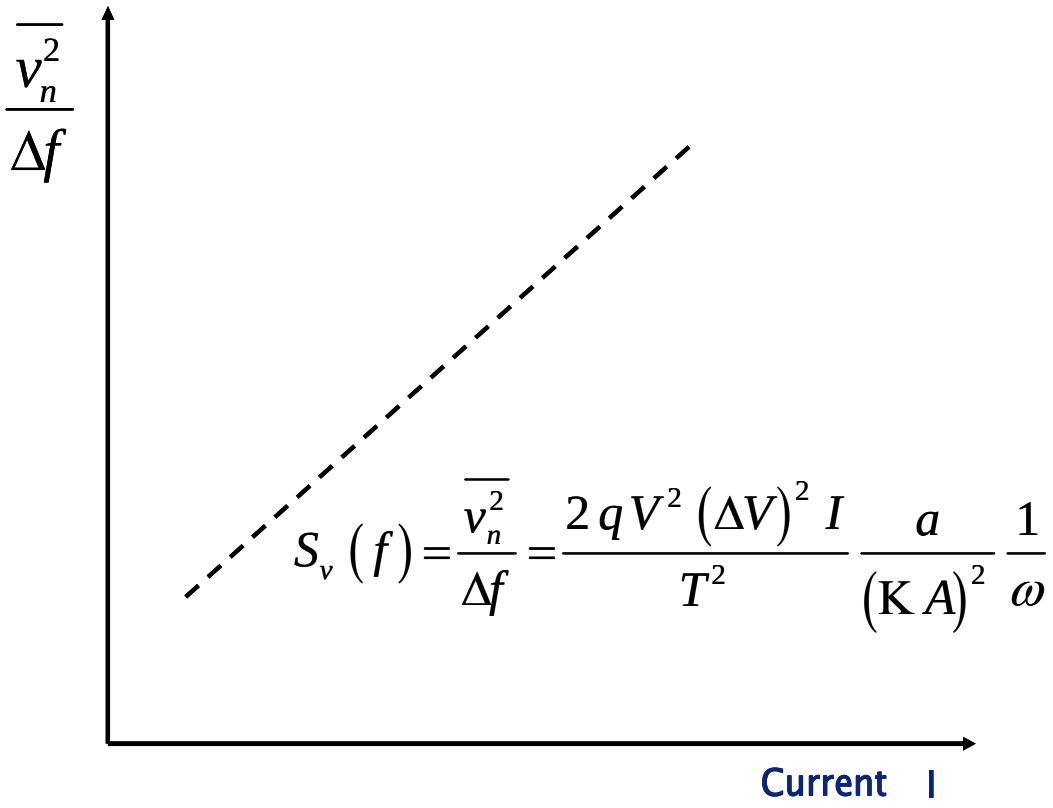


Figure 5.6 Mean square noise voltage across the diode due to power dissipation and temperature fluctuations.

A mean square temperature fluctuation will result in a mean square noise voltage

$$S_v(f) = \frac{\overline{v_n^2}}{\Delta f} = \left( -\frac{E_G}{q} + V_{DC} \right)^2 \frac{\overline{T_n^2}}{T^2} \tag{5.50}$$

and at high frequencies using Eq. (5.29) this becomes

$$S_v(f) = 2qV \frac{\Delta T}{T^2} \frac{a}{\mathrm{K} A d} \frac{1}{\omega} (\Delta V)^2 \tag{5.51}$$

which has a $1/\omega$ frequency dependence. The temperature increase, $\Delta T$ will be $V\ I = \mathrm{K}\ A\ \Delta T / d \quad or\ \ \Delta T = V\ I\ d / (\mathrm{K}\ A)$, so

$$S_v(f) = \frac{\overline{v_n^2}}{\Delta f} = \frac{2\,q\,V^2\,(\Delta V)^2\ I}{T^2} \frac{a}{(\mathrm{K}\ A)^2} \frac{1}{\omega} \tag{5.52}$$

but note that V is a logarithmic function of I and varies slowly. This means that the spectral intensity of the noise is, as shown in Figure 5.6, an approximate linear function of the current and does not vary as the square of DC current. This is a rather unexpected result in the context of Hooge's expression [51]. These results are consistent with recent results on diodes [52] which show the spectral intensity of the 1/f noise varying linearly with the DC bias current. In the case of diodes, because of their low dynamic or internal impedance, it is easy to drive them with a constant DC current and then measure the noise voltage across the diode.

If the diode in Figure 5.5 is replaced by a transistor where the transistor base is by-passed by a large capacitor to keep the base at a fixed potential, the theory developed above can be applied to bipolar junction transistor, too. Figure 5.7 and Figure 5.8 show the cross section of bipolar junction transistor and its bias currents.

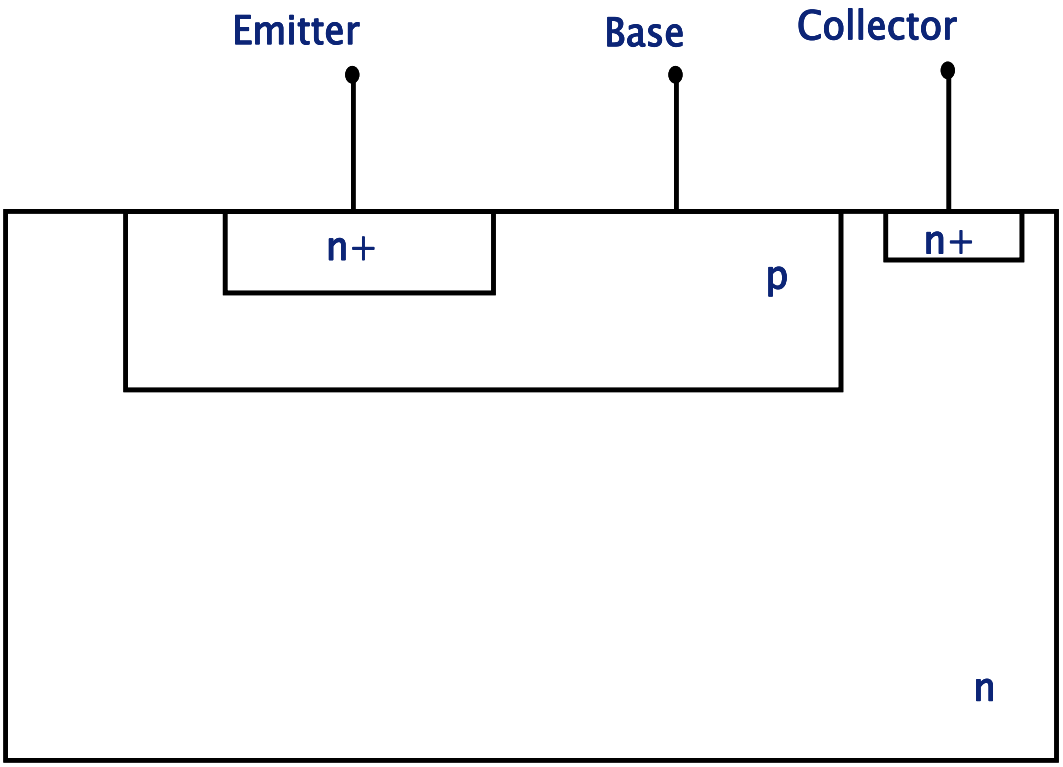


Figure 5.7 Simplified transistor cross section of the bipolar junction transistor.

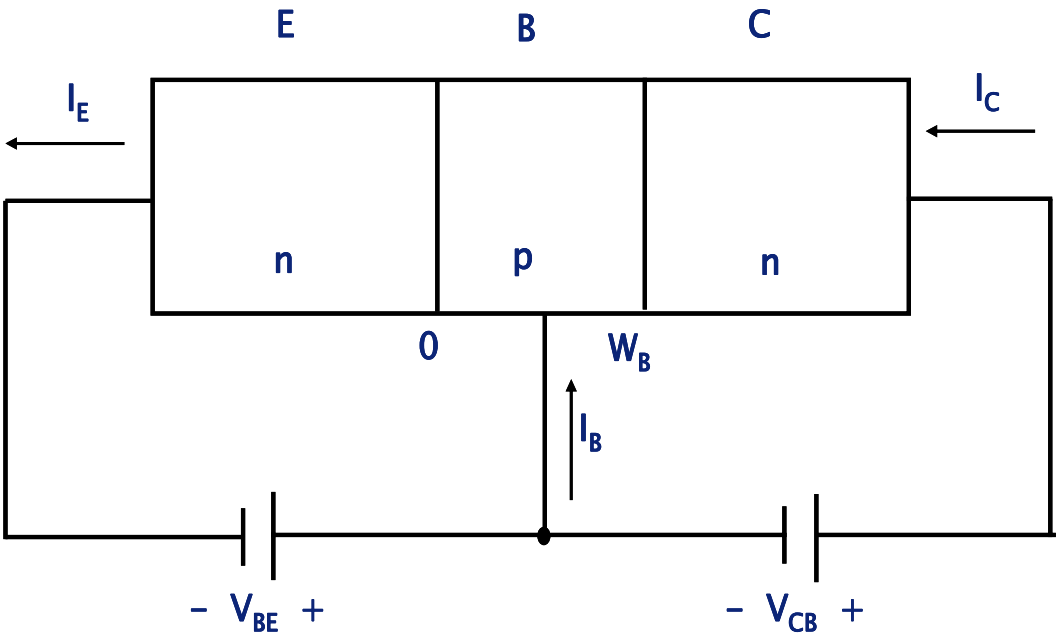


Figure 5.8 Bias condition of the bipolar junction transistor.

Then the modulation of the base-emitter diode temperature will modulate the collector current since

$$I = B\exp\left(-E_G/kT + qV_{DC}/kT\right) \tag{5.53}$$

$$\frac{dI}{dT} = B\exp(-E_G/kT + qV_{DC}/kT).(-E_G/k + qV_{DC}/k).(-1/T^2)$$

$$\frac{dI}{dT} = \left(-\frac{1}{T}\right)\left(\frac{q\Delta V}{kT}\right) I \tag{5.54}$$

$$\left(\frac{dI}{I}\right) = \left(-\frac{dT}{T}\right)\left(\frac{q\Delta V}{kT}\right)$$

$$\left(\frac{dI}{I}\right)^2 = \left(-\frac{dT}{T}\right)^2\left(\frac{q\Delta V}{kT}\right)^2$$

where the mean square fluctuation in temperature from Eq. (5.29) will be determined mostly by power dissipation in the emitter-base junction, and results in temperature increase , $\Delta T$ ,

$$S_T(f) = \frac{\overline{T_n^2}}{\Delta f} = (\frac{1}{\overline{N}})(\Delta T)^2 \frac{2a}{d^2} \frac{1}{\omega}$$

$$= (\frac{1}{\overline{N}})(\Delta T)^2 \frac{2\omega_{cth}}{\omega}, \qquad where \quad \omega_{cth} = \frac{a}{d^2}$$

$$= \frac{q}{I}(\Delta T)^2 .2.\left(\frac{\omega_{cth}}{\omega}\right), \qquad where \quad Flux = \overline{N} q V_{DC} = V_{DC} I, \quad therefore \quad \overline{N} = \frac{I}{q}$$

$$= (\frac{2q}{I})(\Delta T)^2 \left(\frac{\omega_{cth}}{\omega}\right)$$

(5.55)

This results in a mean square fluctuation in the collector current or mean square noise current

$$\overline{i_n^2} = \overline{T_n^2} \frac{I^2}{T^2} \left(\frac{q\Delta V}{kT}\right)^2$$

$$= \frac{2q}{I}(\Delta T)^2 \left(\frac{\omega_{cth}}{\omega}\right) \Delta f \left(\frac{I^2}{T^2}\right) \left(\frac{q\Delta V}{kT}\right)^2 \qquad (5.56)$$

$$= 2qI\Delta f \left(\frac{\Delta V}{(kT/q)}\right)^2 \left(\frac{\Delta T}{T}\right)^2 \left(\frac{\omega_{cth}}{\omega}\right)$$

where now

$$\Delta T = V_{BE} I \frac{d}{KA} \qquad (5.57)$$

is the temperature increase due mostly to power dissipation in the base-emitter junction, and $V_{BE}$ is the base-emitter voltage. Since the output of the common emitter transistor is a current source with high equivalent parallel resistance, measurements on transistors are most easily made of the collector noise current. This again has the 1/f frequency dependence and is simply related to physical parameters of the transistor and heat sink.

### 5.6. Measurement on Light Bulbs, Diodes, and Bipolar Transistors

In order to measure 1/f noise in resistor due to heat conduction, 12v 4watts light bulb was used as a device under test. The temperature of the light bulb increased after the bias voltage was applied. The filament in the light bulb was changed to bright yellow and generated heat. The glass of the light bulb was painted with silver paint to reduce heat radiation to air. Resistance of the light bulb was 4 ohms when the temperature of the light bulb was cold. The resistance was increased to 40 ohms when the light bulb was hot. Figure 5.9 shows simple diagram of the light bulb and its model.

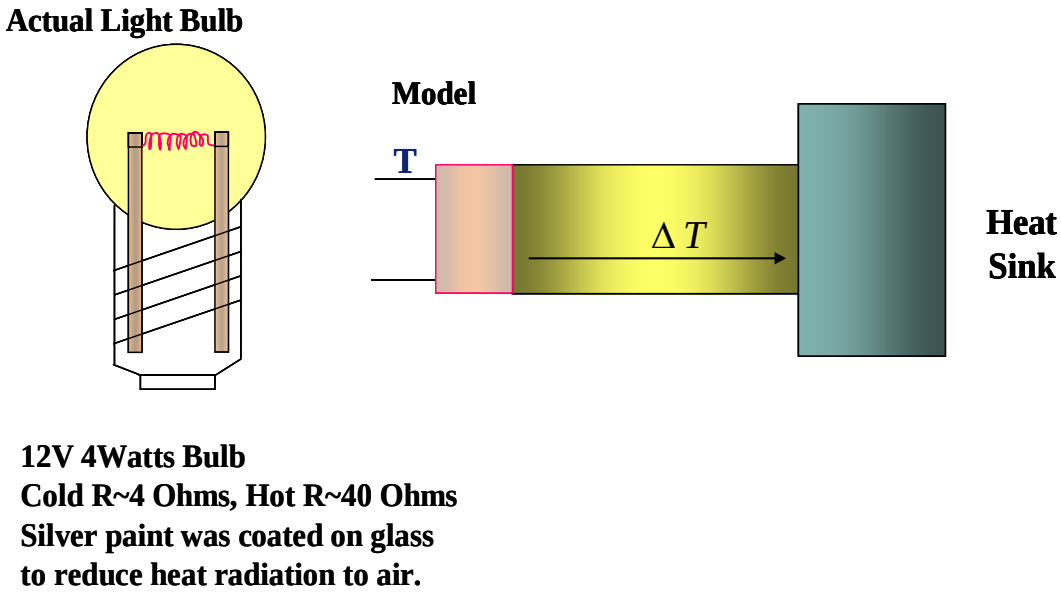


Figure 5.9 Light bulb used for the measurement and its simplified model showing heat conduction.

The heat sink of the light bulb was cooled down to increase the difference of the temperature between heated filament of the light bulb and heat sink. The higher temperature difference can create more heat flux. The noise from the light bulb was amplified with low input impedance amplifier biased with batteries and measured by Princeton Applied Research lock-in amplifier. The measurement setup is given in Figure 5.10.

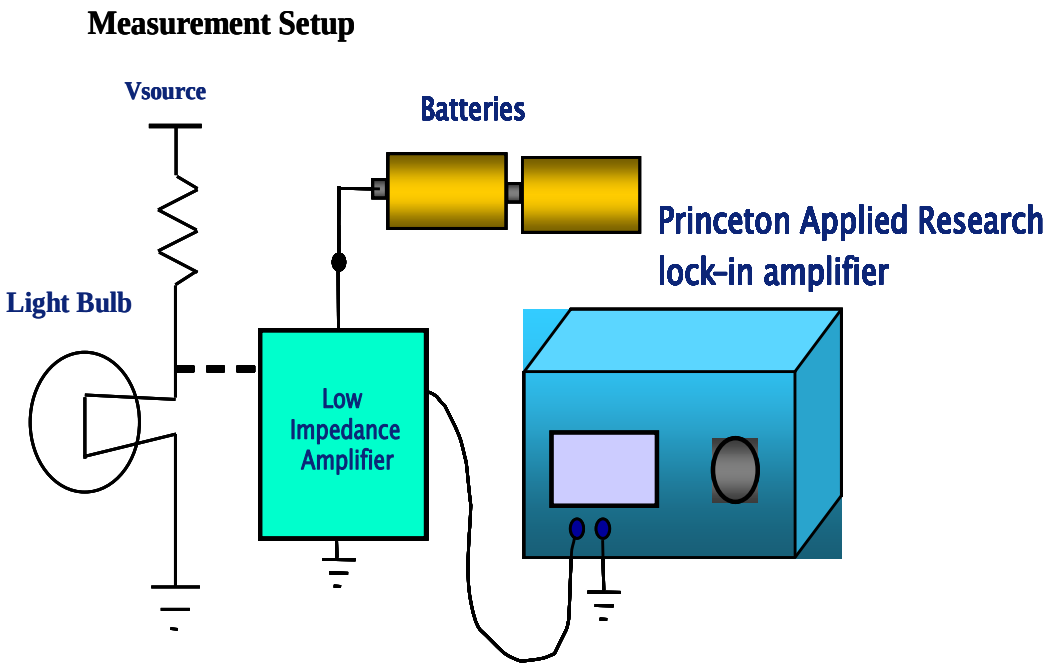


Figure 5.10 Light bulb measurement setup.

Mean square noise current being observed when the filament of the light bulb was heated is given in Figure 5.11. The measured data show noise increase as frequency decreases.

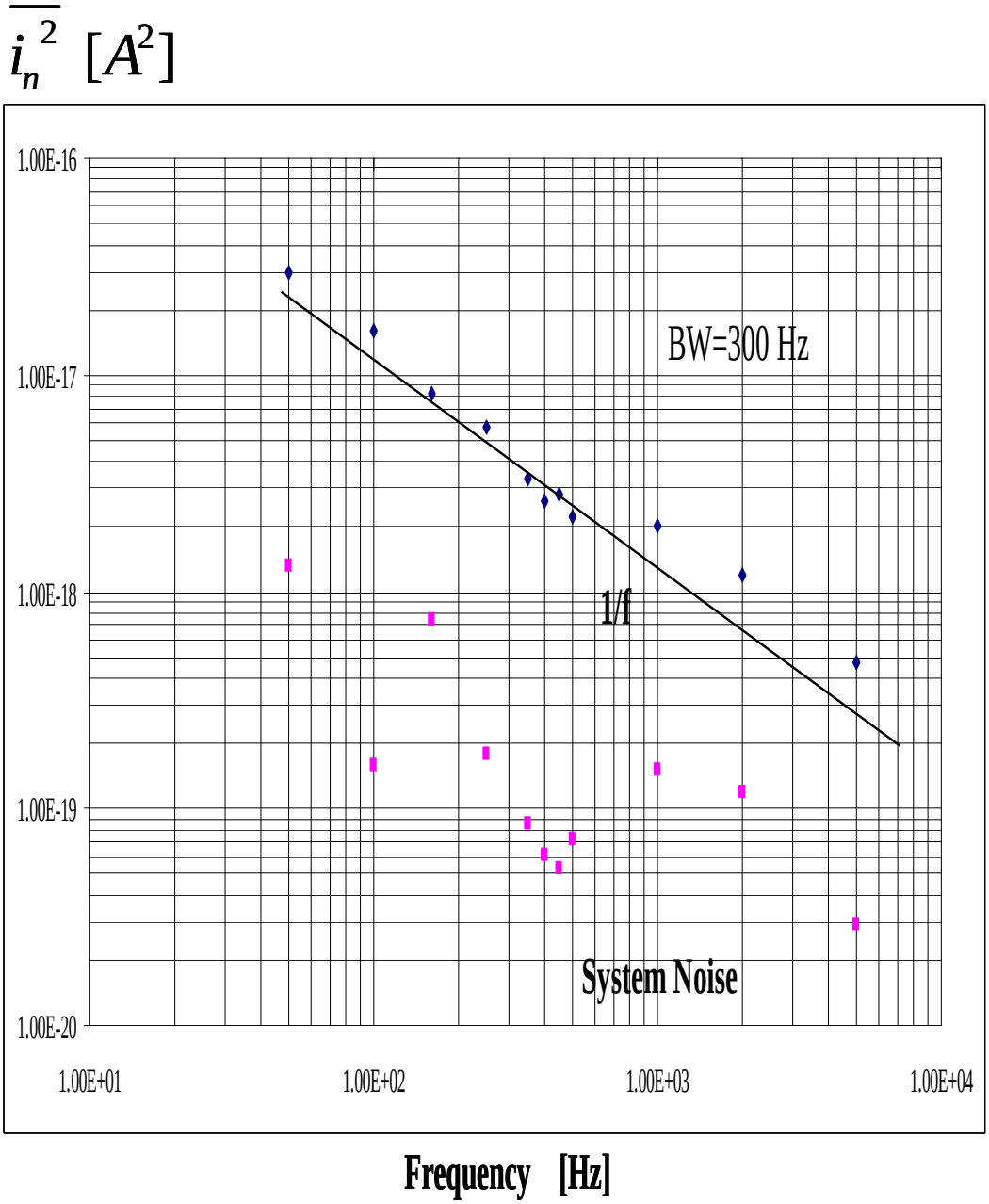


Figure 5.11 Mean square noise current being observed when the light bulb turned on.

The mean square noise voltage versus current from Ge1N34 diode was measured. The measurement was done at 3 KHz frequency and 300 Hz bandwidth. Large DC current was applied to the diode to generate high temperature inside the pn junction. The measured mean square noise voltage was, as shown in Figure 5.12, an approximate linear function of the current and does not vary as the square of DC current. This result is consistent with recent results on laser diodes [53] which show the spectral intensity of the 1/f noise varying linearly with the DC bias current.

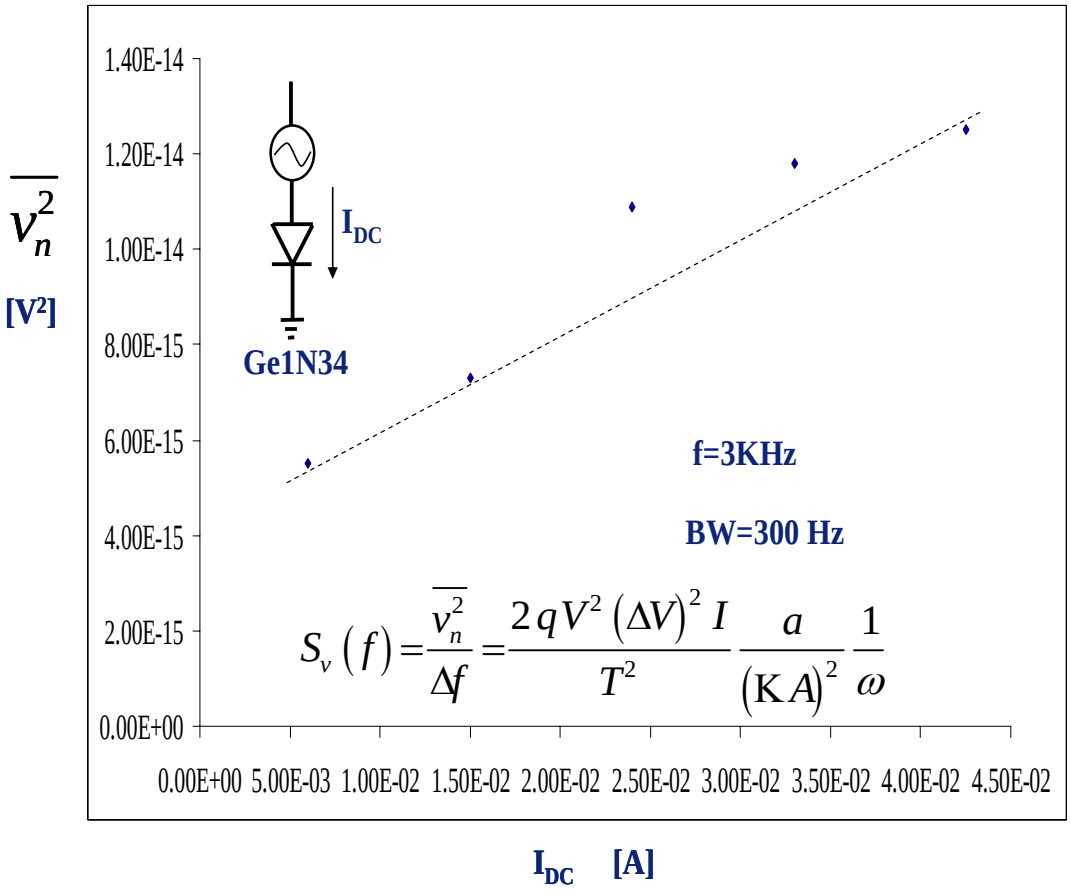


Figure 5.12 Mean square noise voltage measured from diode.

As a demonstration of the concepts of our theoretical results we took a simple plastic or epoxy encapsulated common commercial silicon discrete bipolar transistor.

This device was operated at high currents to generate significant power dissipation in the device and result in a very high junction temperature.

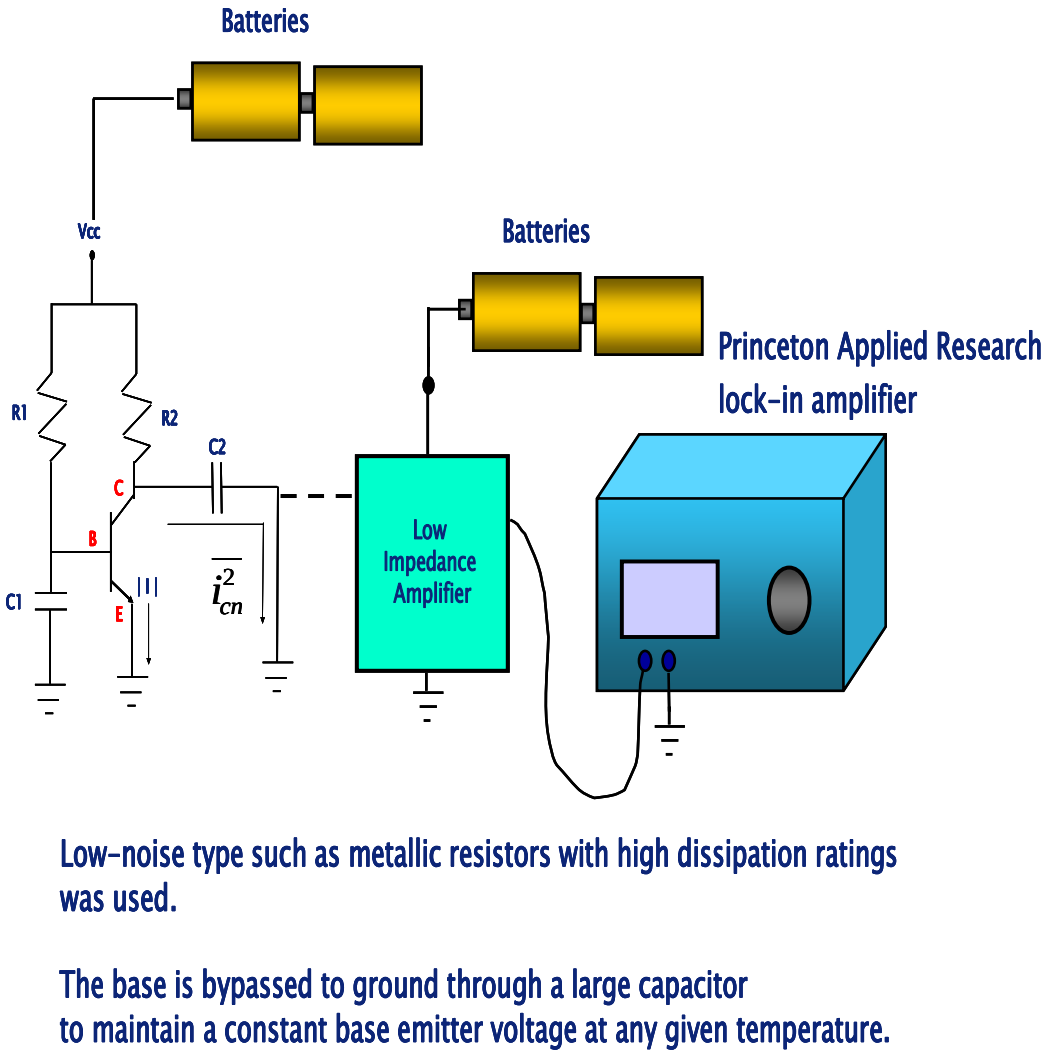


Figure 5.13 Experimental arrangement for measurements of the effect of temperature fluctuations on a bipolar.

Figure 5.13 shows the experimental setup for the 1/f noise measurement of bipolar junction transistor due to temperature fluctuation. Here we used npn transistor with the emitter-base junction to be forward biased and the base-collector junction to be reverse biased. DC biasing is performed with the help of batteries to get noise free power supply to the circuit. All the bias resistor elements used are of low-noise type such as metallic resistors with high dissipation ratings. The base is bypassed to ground through a large capacitor to maintain a constant base emitter voltage at any given temperature. The output is coupled to a common base amplifier with a very low input impedance which acts as an AC short circuit on the output and drives a Princeton Applied Research (PAR) lock-in amplifier being used as narrow bandwidth frequency tunable RMS voltmeter. Although the long-term rms value of noise is a constant, the instantaneous amplitude is totally random, and therefore the meter jitters. For an accurate noise measurement, we can smooth the meter fluctuations by averaging over a long period of time. Averaging was done by using long RC time constant. A small collector resistor is used to maximize power dissipation in the bipolar transistor. The transistor can be biased at a high collector current and the RMS noise current at the collector measured as a function of frequency as is shown in Figure 5.13.

For simplicity it is assumed that the major route of heat dissipation is conduction through the silicon die to a back plane or heat sink, and it is assumed this is a heat sink due to the collector wire contact and convection cooling. This is of course a simplifying assumption, the silicon die is a relatively good heat conductor but there is not a good heat sink, the encapsulated case becomes rather

hot to the touch. These simplifying assumptions are made for a demonstration of concept rather than a detailed description. If the silicon die is about 20 mils thick, and given the thermal diffusivity of silicon is, a=0.9 $cm^2$ /sec, then an estimate of the radian corner frequency, $a/l^2$, results in a frequency of about 349 Hz. Above this frequency the mean square noise current should be expected to have as described by Eq. (5.56) a l/f frequency dependence up to the point where the noise just becomes the mean square shot noise current associated with the DC collector current, $2\,q\,I\,\Delta f$ . Since the junction temperatures become very high the ratio of the temperature difference, $\Delta T$ , over the temperature, T, becomes not too different than one and the ratio of the voltage difference, $\Delta V$ , over the thermal voltage, kT/q, is large or of the order twenty. This latter ratio is, according to the simple ideal diode equation we are using, independent of temperature and can be evaluated at room temperature. In a simple model, the voltage across a diode driven with a constant current is a linearly decreasing function of temperature. These general features are displayed by the experimental results in Figure 5.14, and would result in a l/f noise corner frequency of 100 KHz, below this frequency the noise is l/f noise due to temperature fluctuations in the base emitter junction. While a detailed calculation has not been made since we are using a commercial transistor without controlled experimental conditions and well defined heat sinks the experiment serves as a demonstration of concept in that all of the numerical values are in the correct order of magnitude.

As the power dissipation and junction temperatures are lowered the l/f noise due to temperature fluctuations of the bipolar transistor decreases and is

dominated by other mechanisms or as in our case here background noise of the measurement system.

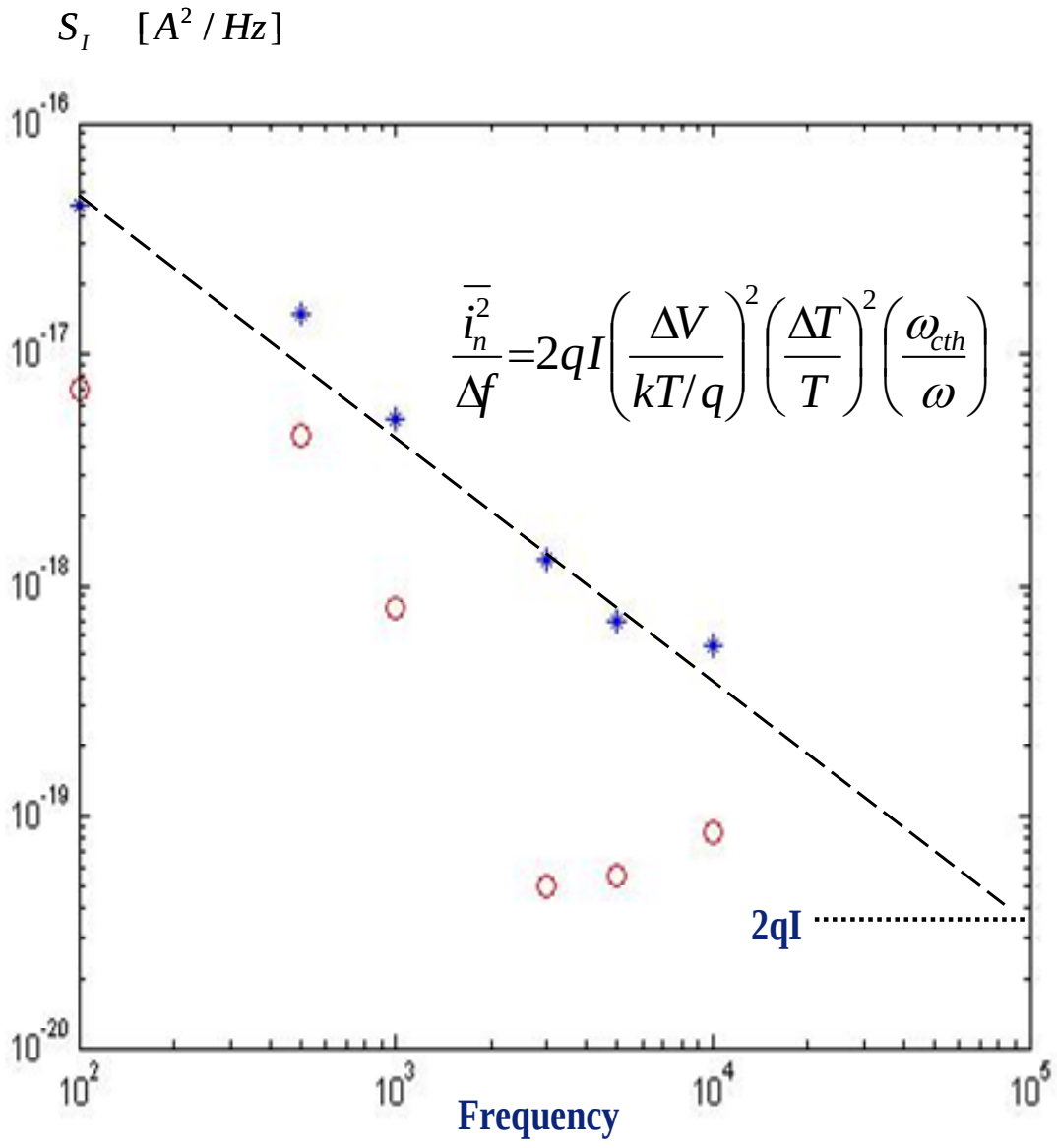


Figure 5.14 Noise current spectrum measured on a bipolar transistor with high power dissipation.

## 5.7. Discussions

The equivalent circuit technique is applied to heat conduction, which is described by the same type of differential equation. It is shown that power dissipation in electron devices will results in temperature fluctuations which are frequency dependent and consequently 1/f noise. The results have been applied to describe measurements on resistive filaments in a vacuum such as in light bulbs where there is significant power dissipation and heat conduction. Mean square noise current from the heated light bulb increased as frequency decreased and showed 1/f noise characteristic. The application of this theory to diode, laser diodes, and transistors with significant power dissipation is considered. The measured mean square noise voltage of diode was an approximate linear function of the current and does not vary as the square of DC current. This result is consistent with recent results on laser diodes which show the spectral intensity of the 1/f noise varying linearly with the DC bias current. The theoretical results presented here and simple experimental results demonstrating the concepts serve to show that temperature fluctuations in electron devices can result in, and are another source of 1/f noise in electron devices.

# 6. CONCLUSIONS

## 6.1. Summary

In this dissertation, we have studied the 1/f noise of resistive filaments in n-GaAs on semi-insulating substrate and compared this to published data. And our own experimental data were presented. The equations derived predict as observed that the noise level increases in proportion to the square of the terminal voltage. We have derived equations to calculate the product $g_{mbg}^2 R$ and to predict the 1/f corner frequency. The 1/f corner frequency calculated corresponds well with that observed in published experimental results. The increase in Hooge's noise parameter with an increase in the voltage drop in the semi-insulating substrate at high electric fields is also predicted. Hooge's parameter in this particular case, is in reality no parameter, but is given by a formula which simply relates the ratio of the charge developed by thermal voltage across the capacitance of the substrate and the implanted charge in the channel with proportional constant which depends on the voltage developed in the semi-insulating substrate and doping concentration of the substrate.

These concepts are probably also applicable to other 1/f noise phenomena which occur in nature, and there may in reality be many analogs in nature. Basically, the concept is that any natural system of large extent, high resistance and some capacity when disturbed will respond by generating 1/f noise, due to their distributed nature.

The equivalent circuit technique is applied to heat conduction, which is described by the same type of differential equation. It is shown that power

dissipation in electron devices will results in temperature fluctuations which are frequency dependent and consequently 1/f noise. The results have been applied to describe measurements on resistive filaments in a vacuum such as in light bulbs where there is significant power dissipation and heat conduction. Mean square noise current from the heated light bulb increased as frequency decreased and showed 1/f noise characteristic. The application of this theory to diode, laser diodes, and transistors with significant power dissipation is considered. The measured mean square noise voltage of diode was an approximate linear function of the current and does not vary as the square of DC current. This result is consistent with recent results on laser diodes which show the spectral intensity of the 1/f noise varying linearly with the DC bias current. The theoretical results presented here and simple experimental results demonstrating the concepts serve to show that temperature fluctuations in electron devices can result in, and are another source of 1/f noise in electron devices.

### 6.2. Future Work

The theory of 1/f noise of semi-insulating material can be extended and applied to analyze and describe the low frequency noise in floating gate devices such as NOR and NAND flash memory. This theory can also be applied to SONOS type flash memory. This theory can be used to analyze the 1/f noise characteristic of the earthquake wave form which results from natural system of large extent, high resistance and some capacity.

As process technology migrates from 90nm to 50nm, more and more transistors and other electronic devices can be fabricated on single silicon die. To meet the specification of many hand held devices, smaller form factor of the package is generally required. Multi chip package (MCP) is one of the favorable solutions to this requirement. Dual silicon dies or quad silicon dies are packaged together and bonded together to the same pins. The significant increase in number of transistor on a single die and the number of silicon dies in one package can create high temperature heat inside the package and silicon. The theory of 1/f noise due to temperature fluctuations can be applied to analyze a noise problem of devices in the multi chip package. The theory can also be used to explain noise problems in nano scale devices which are very sensitive to temperature fluctuations.

# BIBLOGRAPHY

[1] L. Forbes and C. T. Sah, "Application of the distributed equivalent circuit model to semiconductor junctions," IEEE Trans. Electron Devices, vol. ED-16, p. 1036, 1969.

[2] H. F. Friis, “Noise Figures of Radio Receivers,” Proc. IRE, 32, 7, pp. 419-422, 1944.

[3] J. B. Johnson, "Thermal agitation of electricity in conductors," Phys. Rev., vol. 32, pp. 97-109, 1028.

[4] H. Nyquist, “Thermal agitation of electric charge in conductors,” Phys Rev., vol. 32, pp. 110-113, 1928.

[5] A. van der Ziel, "Noise in Solid State Devices and Circuits," p. 19, Wiley Interscience, New York, 1986

[6] K. S. Ralls, W. J. Skocpol, L. D. Jackel, R. E. Howard, L. A. Fetter, R. W. Epworth, and D. M. Tennant, “Discrete resistance switching in submicrometer silicon inversion layers: Individual interface traps and low frequency (1/f?) noise”, Phys. Rev. Lett., vol. 52, no. 3, pp. 228 – 231, Jan. 1984.

[7] M. –H. Tsai, T. P. Ma, T. B. Brook, “Channel length dependence of random telegtraph signal in sub-micron MOSFETs,” IEEE Electron Device Lett., vol. 15, no. 12, pp. 504-506, Dec. 1994.

[8] S. T. Martin, G. P. Li, E. Worley, and J. White, “The gate bias and geometry dependence of random telegraph signal amplitudes,” IEEE Electron Device Lett., vol. 18, no. 9, pp. 444-446, Sep. 1997.

[9] R. Gusmeroli, C. Monzio Compagnoni, A. Riva, A. S. Spinelli, A. L. Lacaita, M. Bonanomi, and A. Visconti, “Defects spectroscopy in SiO2 by statistical random telegraph noise analysis,” IEDM Tech. Dig., pp. 483-486, 2006.

[10] C. Monzio Compagnoni, R. Gusmeroli, A. S. Spinelli, A. L. Lacaita, M. Bonanomi, and A. Visconti, “Statistical model for random telegraph noise in flash memories,” IEEE Trans. Electron Devices , vol. 55, no. 1, pp. 388-395, Jan. 2008.

[11] S. Machlup, “Noise in semiconductors: Spectrum of a tow-parameter random signal,” J. Appl. Phys., 25, pp. 341-343, 1954.

[12] F. N. Hooge, “1/f noise is no surface effect,” Phys. Lett., vol. A-29, p. 139, 1969.

[13] “IRE standards on methods of measuring noise in linear two ports,” Proc. IRE, 48, 1, pp. 60-68, 1960.

[14] C. T. Sah, " The equivalent circuit model in solid-state electronics - Part I: The single energy-level defect centers," Proc. of the IEEE, vol. 55, p. 654, 1967.

[15] C. T. Sah, " The equivalent circuit model in solid-state electronics - Part II: The multiple energy-level defect centers," Proc. of the IEEE, vol. 55, p. 672, 1967.

[16] L. Forbes and C. T. Sah, "Application of the distributed equivalent circuit model to semiconductor junctions," IEEE Trans. Electron Devices, vol. ED-16, p. 1036, 1969.

[17] L. Forbes and B. Rastegar, "A desk-top-computer based calculation of high frequency MOS C-V curves," IEEE Trans. Electron Devices, vol. ED-34, p. 427, 1987.

[18] L. Forbes, “On the theory of the 1/f noise of semi-insulating materials,” IEEE Trans. Electron Devices, vol. 42, p. 1866, Oct. 1995.

[19] T. Musha, in Proc. 1/f Noise Symp., p. 49, 1977.

[20] V. Radeka, “1/|f| noise in physical measurements,” IEEE Trans. Nucl. Sci., vol. NS-16, p. 17, Oct. 1969.

[21] M. S. Keshner, “1/f noise,” Proc. IEEE, vol. 70, p. 212, 1982.

[22] M. Tacano and Y. Sugiyama, "1/f noise in GaAs filaments", IEEE Trans. Electron Devices, vol. ED-38, p. 2548, 1991.

[23] L. Forbes, K. T. Yan and M. S. Choi, "1/f noise corner frequency of FET's on semi-insulating substrates," Ext. Abs. US Conference on GaAs Manufacturing Technology, New Orleans, p. 52, May 1995.

[24] K. T. Yan and L. Forbes, “A model for the 1/f noise corner frequency of FET’s on semi-insulating substrates based on bulk phenomena,” Solid-State Electronics, in press.

[25] F. N. Hooge, "1/f noise is no surface effect," Phys. Lett. vol. 29, p. 139, 1969

[26] F. N. Hooge, "Discussion of recent experiments on 1/f Noise," Physica vol. 60, p. 130, 1972

[27] A. van der Ziel, "Flicker Noise in Electronic Devices," Advances in Electronics and Electron Physics (Edited by L. Martin) p. 225, Academic Press, New York, 1979

[28] H. I. Hanafi and A. van der Ziel, "Flicker noise in $Hg_{1-x}Cd_xTe$," Physica vol. B94, p. 351, 1978.

[29] T. G. M. Kleinpenning, "1/f noise in thermo emf of intrinsic and extrinsic semiconductors," Physica, vol. 77, p. 78, 1974.

[30] T. G. M. Kleinpenning, "1/f noise in solid state single injection diodes," Physica vol. 94B, p. 141, 1978.

[31] F. N. Hooge and L. K. Vandamme, "Lattice scattering causes 1/f noise," Phys. Lett. vol. A66, p. 315, 1978.

[32] T. G. M. Kleinpenning, "1/f noise in p-n diodes," Physica, vol. 98B, p. 289,1980.

[33] T. G. M. Kleinpenning, "1/f noise of hot carriers in n-type silicon," Physica, vol. 103B, p. 340, 1981.

[34] K. M. van Vilet and R. J. J. Zijlstra, "On mobility fluctuations in 1/f noise," Physica, vol. 111B, p. 321, 1981.

[35] F. N. Hooge, "On Expressions for 1/f noise in mobility," Physica, vol. 114B, p. 391, 1982.

[36] J. Bisschop, "On 1/f noise originating from mobility fluctuations," Physica, vol. 119B, p. 290, 1983.

[37] C. H. Suh and A. van der Ziel and R. P. Jindal, "1/f noise in GaAs MESFETs," Solid-State Electron., vol. 24, p.717, 1981.

[38] M. Tacano, H. Tanoue and Y. Sugiyama, "Dependence of Hooge parameter of compound semiconductors on temperature," Jpn. J. Appl. Phys. vol. 31, p. L316, 1992.

[39] F. N. Hooge and M. Tacano, "Experimental studies of 1/f noise in n-GaAs," Physica, vol. B190, p. 145, 1993.

[40] L. Ren and F. N. Hooge, "Temperature dependence of 1/f noise in epitaxial n-type GaAs," Physica, vol. B176, p. 209, 1992.

[41] G.M. Martin, J. P. Farges, G. Jacob, and J. P. Hallais, "Compensation mechanisms in GaAs," J. Appl. Phys. vol. 51, No. 5, p. 2840, 1980.

[42] L. Forbes, K.T. Yan and M.S. Choi, "1/f noise corner frequency of FET's on semi-insulating substrates," Ext. Abs. U.S. Conf. on GaAs Manufacturing Technology (MANTECH), New Orleans, pp. 52-55, 1995.

[43] K.T. Yan and L. Forbes, "Design for and the control of channel and 1/f noise in GaAs MESFET's," Int'l. Symp. on the Physical and Failure Analysis of Integrated Circuits, Singapore, pp. 164-168, 1995.

[44] K.T. Yan and L. Forbes, "1/f bulk phenomena noise theory for GaAs MESFET's," IEEE TENCON on Microelectronics and VLSI, Hong Kong, pp. 111-114, 1995.

[45] L. Forbes, M.S. Choi and L. Forbes, "1/f noise of GaAs resistors on semi-insulating substrates," IEEE Trans. on Electron Devices, vol. ED-43, pp. 622-627, 1996.

[46] L. Forbes and M.S. Choi, "l/f noise due to temperature fluctuations in heat condition," Ext. Abst. Device Research Conference, Santa Barbara, pp. 46-47, 1996.

[47] C. Kittel and H. Kroemer, Thermal Physics, 2nd Ed., New York: Freeman, p. 424, 1980.

[48] K. M. van Vilet, R. R. Schmidt, and A. van def Ziel, "Temperature-fluctuation noise of thin films supported by a ssubstrate," J. Appl. Phys. vol. 51, no. 6, pp. 2947-2956, 1980.

[49] A. Diaz-Guilera and J. M. Rubi, "Internal and external fluctuations around nonequilibrium steady states in one-dimensional heat-conduction problems," Phys. Rev. A, vol. 34, no. 1, pp. 462-467, 1986.

[50] H.P. Breuer and F. Petruccione, "A master equation approach to fluctuating hydrodynamics: heat conduction," Phys. Lett. A, vol. 185, no. 4, pp. 385-389, 1994.

[51] F.N. Hooge, "l/f noise is no surface effect," Phys. Lett., vol. 29A, No. 3, pp. 130-140, 1969.

[52] S. Yang, T. Mizunami, and K. Takagi, “Current dependence of 1/f noise in junction diodes,” Japan J. Appl. Phys., vol. 31, No. 6A, pp. 1752-1755, 1992.

[53] S. Yang, T. Sasaki, T. Mizunami, and K. Takagi, “Measurements on low frequency fluctuation in laser diodes,” IEEE Trans. on Electron Devices, vol. 41, No. 11, pp. 2162-2164, 1994.